[11] P.D. Vermeer, L.A. Einwalter, T.O. Moninger, T. Rokhlina, J.A. Kern, J. Zabner, M.J. Welsh, Segregation of receptor and ligand regulates activation of epithelial growth factor receptor, Nature 422 (2003) 322–326.
[12] P.J. Morin, Claudin proteins in human cancer: promising new targets for diagnosis and therapy, Cancer Res. 65 (2005) 9603–9606.
[13] M. Furuse, S. Tsukita, Claudins in occluding junctions of humans and flies, Trends Cell Biol. 16 (2006) 181–188.
[14] S.L. Kominsky, Claudins: emerging targets for cancer therapy, Expert Rev. Mol. Med. 8 (2006) 1–11.
[15] J. Katahira, N. Inoue, Y. Horiguchi, M. Matsuda, N. Sugimoto, Molecular cloning and functional characterization of the receptor for *Clostridium perfringens* enterotoxin, J. Cell Biol. 136 (1997) 1239–1247.
[16] S.L. Kominsky, M. Vali, D. Korz, T.G. Gabig, S.A. Weitzman, P. Argani, S. Sukumar, *Clostridium perfringens* enterotoxin elicits rapid and specific cytolysis of breast carcinoma cells mediated through tight junction proteins claudin 3 and 4, Am. J. Pathol. 164 (2004) 1627–1633.
[17] A.D. Santin, S. Cane, S. Bellone, M. Palmieri, E.R. Siegel, M. Thomas, J.J. Roman, A. Burnett, M.J. Cannon, S. Pecorelli, Treatment of chemotherapy-resistant human ovarian cancer xenografts in C.B-17/SCID mice by intraperitoneal administration of *Clostridium perfringens* enterotoxin, Cancer Res. 65 (2005) 4334–4342.
[18] P. Michl, M. Buchholz, M. Rolke, S. Kunsch, M. Lohr, B. McClane, S. Tsukita, G. Leder, G. Adler, T.M. Gress, Claudin-4: a new target for pancreatic cancer treatment using *Clostridium perfringens* enterotoxin, Gastroenterology 121 (2001) 678–684.
[19] N. Sonoda, M. Furuse, H. Sasaki, S. Yonemura, J. Katahira, Y. Horiguchi, S. Tsukita, *Clostridium perfringens* enterotoxin fragment removes specific claudins from tight junction strands: Evidence for direct involvement of claudins in tight junction barrier, J. Cell Biol. 147 (1999) 195–204.
[20] R.J. Collier, *Diphtheria* toxin: mode of action and structure, Bacteriol. Rev. 39 (1975) 54–85.
[21] D. Leong, K.D. Coleman, J.R. Murphy, Cloned fragment A of *diphtheria* toxin is expressed and secreted into the periplasmic space of *Escherichia coli* K12, Science 220 (1983) 515–517.
[22] P.O. Falnes, K. Sandvig, Penetration of protein toxins into cells, Curr. Opin. Cell Biol. 12 (2000) 407–413.
[23] P.C. Hanna, T.A. Mietzner, G.K. Schoolnik, B.A. McClane, Localization of the receptor-binding region of *Clostridium perfringens* enterotoxin utilizing cloned toxin fragments and synthetic peptides. The 30 C-terminal amino acids define a functional binding region, J. Biol. Chem. 266 (1991) 11037–11043.
[24] M. Yamaizumi, E. Mekada, T. Uchida, Y. Okada, One molecule of *diphtheria* toxin fragment A introduced into a cell can kill the cell, Cell 15 (1978) 245–250.
[25] F. Foss, Clinical experience with denileukin diftitox (ONTAK), Semin. Oncol. 33 (2006) S11–S16.
[26] A.E. Frankel, D.R. Fleming, P.D. Hall, B.L. Powell, J.H. Black, C. Leftwich, R. Gartenhaus, A phase II study of DT fusion protein denileukin diftitox in patients with fludarabine-refractory chronic lymphocytic leukemia, Clin. Cancer Res. 9 (2003) 3555–3561.
[27] A.E. Frankel, B.L. Powell, P.D. Hall, L.D. Case, R.J. Kreitman, Phase I trial of a novel *diphtheria* toxin/granulocyte macrophage colony-stimulating factor fusion protein (DT 388GMCSF) for refractory or relapsed acute myeloid leukemia, Clin. Cancer Res. 8 (2002) 1004–1013.
[28] A. Takahashi, M. Kondoh, A. Masuyama, M. Fujii, H. Mizuguchi, Y. Horiguchi, Y. Watanabe, Role of C-terminal regions of the C-terminal fragment of *Clostridium perfringens* enterotoxin in its interaction with claudin-4, J. Control. Release 108 (2005) 56–62.
[29] J.S. Bonifacino, L.M. Traub, Signals for sorting of transmembrane proteins to endosomes and lysosomes, Annu. Rev. Biochem. 72 (2003) 395–447.
[30] A.I. Ivanov, A. Nusrat, C.A. Parkos, Endocytosis of epithelial apical junctional proteins by a clathrin-mediated pathway into a unique storage compartment, Mol. Biol. Cell 15 (2004) 176–188.
[31] M. Matsuda, A. Kubo, M. Furuse, S. Tsukita, A peculiar internalization of claudins, tight junction-specific adhesion molecules, during the intercellular movement of epithelial cells, J. Cell Sci. 117 (2004) 1247–1257.
[32] C. Ebihara, M. Kondoh, N. Hasuike, M. Harada, H. Mizuguchi, Y. Horiguchi, M. Fujii, Y. Watanabe, Preparation of a claudin-targeting molecule using a C-terminal fragment of *Clostridium perfringens* enterotoxin, J. Pharmacol. Exp. Ther. 316 (2006) 255–260.

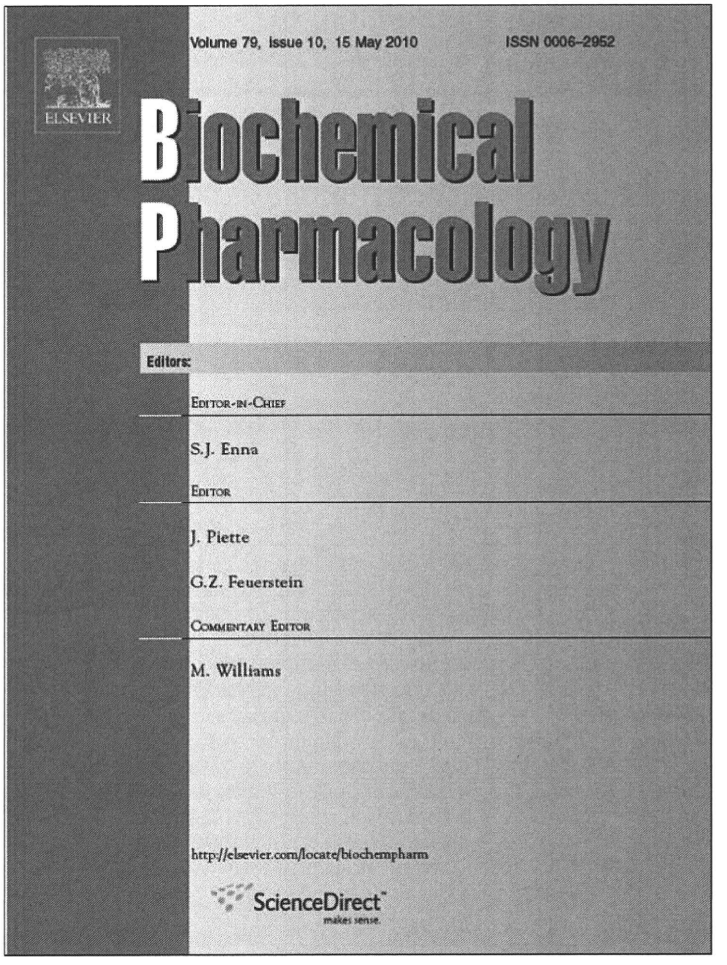

Biochemical Pharmacology 79 (2010) 1437–1444

Contents lists available at ScienceDirect

Biochemical Pharmacology

journal homepage: www.elsevier.com/locate/biochempharm

A claudin-4 modulator enhances the mucosal absorption of a biologically active peptide

Hiroshi Uchida [a,*], Masuo Kondoh [b,**], Takeshi Hanada [a], Azusa Takahashi [b], Takao Hamakubo [c], Kiyohito Yagi [b]

[a] Department of Biopharmaceuticals Research, Biopharma Center, Asubio Pharma Co., Ltd., Gunma, Japan
[b] Laboratory of Bio-Functional Molecular Chemistry, Graduate School of Pharmaceutical Sciences, Osaka University, Osaka, Japan
[c] Department of Molecular Biology and Medicine, Research Center for Advanced Science and Technology, The University of Tokyo, Tokyo, Japan

ARTICLE INFO

Article history:
Received 21 December 2009
Accepted 12 January 2010

Keywords:
Mucosal absorption
Claudin
Paracellular route
Tight junction
Epithelial barrier

ABSTRACT

Biologics, such as peptides, proteins and nucleic acids, are emerging pharmaceuticals. Passage across the epithelium is the first step in the absorption of biologics. Tight junctions (TJ) function as seals between adjacent epithelial cells, preventing free movement of solutes across the epithelium. We previously found that modulation of a key TJ component, claudin-4, is a potent method to enhance jejunal absorption when we used dextran as a model drug and the C-terminal fragment of *Clostridium perfringens* enterotoxin (C-CPE) as a claudin-4 modulator. Here, we investigated whether the claudin-4 modulator enhances jejunal, nasal and pulmonary absorption of a biologics human parathyroid hormone derivative, hPTH(1-34). The claudin-4 modulator enhanced nasal but not jejunal and pulmonary absorption of hPTH(1-34). C-CPE is hydrophobic with low solubility of less than 0.3 mg/ml, but deletion of 10 amino acids at the N-terminal of C-CPE increased its solubility by 30-fold. Moreover, the N-terminal truncated C-CPE bound to claudin-4, modulated the TJ-barrier and enhanced jejunal absorption of dextran. The N-terminal-truncated C-CPE also enhanced jejunal and pulmonary absorption of hPTH(1-34). This report is the first to indicate that a claudin-4 modulator may be a promising enhancer of the jejunal, pulmonary and nasal absorption of a peptide drug.

1. Introduction

Recent progress in genomic and proteomic technologies has yielded some new biologics, such as peptides, proteins and nucleic acids, as pharmaceutical candidates. Passage across the mucosal epithelium of the intestine, nose and lung is the first step in drug absorption. However, most biologics are hydrophilic molecules that are poorly absorbed by the mucosa. Although injection is a compelling route for the administration of biologics, a transmucosal delivery system would be an ideal administration route for biologics because it is noninvasive and therefore would provide a higher quality of life to patients. However, it is difficult to develop a transmucosal delivery system since the epithelium plays a pivotal role in the barrier separating the inside of the body from the outside environment.

Tight junctions (TJ) exist between adjacent epithelial cells and seal the paracellular space, preventing free movement of solutes [1]. To facilitate drug absorption, modulators of the epithelial barrier have been investigated since 1960s [2,3]. Many TJ modulators, such as fatty acids, bile salts, a polysaccharide and a toxin fragment, have been developed [4–6]. However, the biochemical structures of TJs remained uncharacterized until 1998, and a drug absorption enhancer based on TJ-components has never been fully developed [7]. Occludin, a 65-kDa tetra-transmembrane protein, was the first TJ-structural component to be identified [8]. Claudin, a 23-kDa integral membrane protein bearing tetra-transmembrane domains, is the functional component of the TJ-barrier [9,10]. The claudin family consists of 24

Abbreviations: TJ, tight junction; C-CPE, the C-terminal fragment of *Clostridium perfringens* enterotoxin; C-CPE184, C-terminal fragment of *Clostridium perfringens* enterotoxin from 184 to 319 amino acids; hPTH, human parathyroid hormone; CPE, *Clostridium perfringens* enterotoxin; DDM, n-Dodecyl-β-D-maltoside; EDC, N-ethyl-N′-(3-dimethylaminopropyl)-carbodiimide; NHS, N-hydroxysuccinimide; C-CPE194, C-terminal fragment of *Clostridium perfringens* enterotoxin from 194 to 319 amino acids; C-CPE205, C-terminal fragment of *Clostridium perfringens* enterotoxin from 205 to 319 amino acids; PBS, phosphate-buffered saline; SDS-PAGE, sodium dodecyl sulfate-polyacrylamide gel electrophoresis; BV, budded baculovirus; TBS, Tris-buffered saline; ELISA, enzyme-linked immunosorbent assay; SPR, surface plasmon resonance; TEER, transepithelial electric resistance; FD-4, fluorescein isothiocyanate-dextran with a molecular weight of 4 kDa; AUC, the area under the plasma concentration; BA, bioavailability.

* Corresponding author at: Department of Biopharmaceuticals Research, Biopharma Center, Asubio Pharma Co., Ltd., Gunma 370-0503, Japan. Tel.: +81 276 86 7359; fax: +81 276 86 5787.
** Corresponding author at: Laboratory of Bio-Functional Molecular Chemistry, Graduate School of Pharmaceutical Sciences, Osaka University, Suita, Osaka 565-0871, Japan. Tel.: +81 6 6879 8196; fax: +81 6 6879 8199.
E-mail addresses: uchida.hiroshi.b3@asubio.co.jp (H. Uchida), masuo@phs.osaka-u.ac.jp (M. Kondoh).

0006-2952/$ – see front matter © 2010 Elsevier Inc. All rights reserved.
doi:10.1016/j.bcp.2010.01.010

members with different barrier functions among tissues. For example, claudin-1 and -5 function in the epidermal barrier and blood-brain barrier, respectively [11,12]. Claudin is heterogeneously expressed in epithelial cells of the gut, lung and nose [13–15]. The extracellular loop domains of claudin between adjacent cells are estimated to be involved in the paracellular tightness of the cleft between cells, resulting in prevention of solute movement by the formation of TJs [16,17]. Therefore, a molecule that can bind to the extracellular loop domain of claudin may be a novel type of mucosal-absorption enhancer.

The 35-kDa *Clostridium perfringens* enterotoxin (CPE) causes food poisoning in humans [18]. The receptor for CPE is claudin-4 [10]. The C-terminal fragment of CPE (amino acids 184–319; C-CPE184) is the receptor-binding region of CPE. Treatment of cells with C-CPE184 disrupted the TJ-barrier through its interaction with the second extracellular loop of claudin-4, indicating that C-CPE184 is a claudin-4 modulator [10,19,20]. We previously found that C-CPE184 enhanced the jejunal absorption of dextran (molecular mass, 4 kDa) over 400-fold compared with a clinically used absorption enhancer, sodium caprate, and that deletion of the claudin-4-binding region in C-CPE attenuated the absorption-enhancing effect of C-CPE [21]. Claudin-4 is also expressed in nasal and pulmonary epithelial cells [14,15,22]. Thus, a claudin-4 modulator may be a promising candidate for the enhancement of not only jejunal absorption but also pulmonary and nasal absorption of biologics; however, the ability of a claudin modulator to enhance the mucosal absorption of biologics has not yet been investigated.

In the present study, we investigated whether claudin-4 modulation enhanced jejunal, nasal and pulmonary absorption of a peptide drug, human parathyroid hormone derivative (hPTH(1-34)) using C-CPE184 and its derivatives. We found that a claudin-4 modulator was a novel mucosal-absorption enhancer of a peptide drug.

2. Materials and methods

2.1. Materials

Human parathyroid hormone derivative (hPTH(1-34)) was prepared as described previously [23]. n-Dodecyl-β-D-maltoside (DDM) was purchased from Dojindo Laboratories (Kumamoto, Japan). Anti-claudin antibodies and anti-his-tag antibody were obtained from Invitrogen (Carlsbad, CA) and EMD Chemicals Inc. (Darmstadt, Germany), respectively. CM5 sensor chips, amine-coupling reagents (N-ethyl-N′-(3-dimethylaminopropyl)-carbodiimide (EDC), N-hydroxysuccinimide (NHS), and ethanolamine–HCl) and HBS-EP+ (10 mM HEPES, pH 7.4, 150 mM NaCl, 3 mM EDTA and 0.05% surfactant P20) were obtained from GE Healthcare (Buckinghamshire, UK). All reagents used were of research grade.

2.2. Preparation of N-terminal-truncated C-CPE derivatives

We prepared expression vectors of N-terminal region-truncated C-CPE184 (amino acids 184–319). These vectors expressed amino acids 194–319 (C-CPE194), 205–319 (C-CPE205), 212–319 (C-CPE212), 219–319 (C-CPE219) and 224–319 (C-CPE224). Insert fragments of each C-CPE mutant were amplified from C-CPE184 cDNA (kindly provided by Dr. Y. Horiguchi, Osaka University) by polymerase chain reaction with forward primers (5′-ATGCTCGAGGATATAGAAAAAGAAATCCTT-3′ for C-CPE194, 5′-ATGCTCGAGGCTACAGAAAGATTAAATTTAACTG-3′ for C-CPE205, 5′-ATGGGGGAGGCTACAGAAAGATTAAATTTAACTG-3′ for C-CPE212, 5′-ATGCTCGAGGCTGAAGCCCAAGATTAAATTTAACTG-3′ for C-CPE219, 5′-ATGCTCGATCTATGAAGATTAAATTTAACTG-3′ for C-CPE224) and a common reverse primer (5′-TTTGCTAGCTAAGATTCTATATTTTTGTCC-3′). The resultant C-CPE fragments were cloned into the pET16b vector. The plasmids were transduced into *E. coli* BL21 (DE3), and protein expression was stimulated by the addition of isopropyl-1-thio-β-D-galactoside. The cell lysates were applied to HisTrap™ HP (GE Healthcare), and C-CPEs were eluted with imidazole. The solvent was exchanged with phosphate-buffered saline (PBS) by gel filtration, and the purified proteins were stored at −80 °C until use. Purification of the proteins was confirmed by sodium dodecyl sulfate-polyacrylamide gel electrophoresis (SDS-PAGE) followed by staining with Coomassie Brilliant Blue. C-CPEs were quantified by using a BCA protein assay kit (Thermo Fisher Scientific Inc., Rockford, IL) with bovine serum albumin as a standard.

2.3. Preparation of claudin-displaying budded baculovirus (BV)

Claudin-displaying BV was prepared as described previously [24]. Briefly, mouse claudin-1 and -4 cDNA fragments were cloned into the baculoviral transfer vector pFastBac1 (Invitrogen). Recombinant baculoviruses were generated by using the Bac-to-Bac system according to the manufacturer's instructions (Invitrogen). Sf9 cells were cultured in Grace's Insect medium (Invitrogen) containing 10% FBS at 27 °C and infected with the recombinant baculovirus. Seventy-two hours after infection, the BV fraction was isolated from the culture supernatant of the infected Sf9 cells by centrifugation at 40,000 × *g* for 25 min. The pellets of the BV fraction were suspended in Tris-buffered saline (TBS) containing protease inhibitor cocktail (Sigma–Aldrich, St. Louis, MI) and then stored at 4 °C. The expression of claudins in the BV fraction was confirmed by SDS-PAGE and immunoblot with antibodies against claudins.

2.4. Enzyme-linked immunosorbent assay (ELISA) with claudin-displaying BV

The claudin-displaying BV were diluted with TBS and adsorbed to the wells of 96-well immunoplates (Nunc, Roskilde, Denmark) overnight at 4 °C. The wells were washed with PBS and blocked with TBS containing 1.6% BlockAce (Dainippon Sumitomo Pharma, Osaka, Japan) for 2 h at room temperature. C-CPE or C-CPE derivatives were added to the wells and incubated for an additional 2 h at room temperature. The wells were washed with PBS and incubated with anti-his-tag antibody for 2 h at room temperature. The immuno-reactive proteins were detected by a horseradish peroxidase-labeled secondary antibody with 3,3′,5,5′-tetramethylbenzine as a substrate. The reaction was terminated by the addition of 0.5 M H_2SO_4, and the immuno-reactive proteins were measured at 450 nm.

2.5. Preparation of recombinant claudin-4 protein

Recombinant claudin-4 protein was prepared by using Sf9 cells infected with recombinant baculovirus, as previously reported [25,26]. Briefly, the C-terminal his-tagged claudin-4 cDNA fragment was cloned into pFastBac1, and recombinant baculovirus was generated by using the Bac-to-Bac baculovirus expression system. Sf9 cells were infected with the recombinant baculovirus. After 52–56 h of infection, the cells were harvested by centrifugation. The cells were washed with PBS and were resuspended in 10 mM Hepes, pH 7.4, 120 mM NaCl with protease inhibitor tablets (Complete Mini, EDTA-free, Roche Applied Science (Indianapolis, IN)), 1 mM phenylmethylsulfonyl fluoride and 20 units/ml DNase I. The cells were lysed by the addition of 2% of DDM and were then centrifuged. The resultant supernatant was applied to HisTrap™ HP, and claudin-4 was eluted with imidazole. The solvent for claudin-4 was exchanged to PBS containing 0.2% DDM by gel

filtration with a HiTrap Desalting column (GE Healthcare). Purification of claudin-4 was confirmed by SDS-PAGE followed by staining with Coomassie Brilliant Blue.

2.6. Surface plasmon resonance (SPR) analysis

SPR measurements were performed with a Biacore T100 instrument (GE Healthcare). Amine-coupling chemistry was used to immobilize claudin-4 at 25 °C on a CM5 sensor chip surface docked in a Biacore T100 and equilibrated with HBS-EP+. The carboxymethyl surface of the CM5 chip was activated for 2 min with a 1:1 ratio of 0.4 M EDC and 0.1 M NHS at a flow rate of 10 μl/min. Claudin-4 was diluted to 2.5 μg/ml in 10 mM MES buffer (pH 6.5) and injected for 2 min over the surface at a flow rate of 10 μl/min. Excess activated groups were blocked by a 5-min injection of 1 M ethanolamine (pH 8.5) at a flow rate of 10 μl/min. Approximately 1000 RU of claudin-4 was immobilized by using this protocol. Single-cycle kinetics experiments were performed at 25 °C with a flow rate of 30 μl/min [27]. C-CPE or its derivatives were serially diluted (1.25, 2.5, 5, 10 and 20 nM) in running buffer (HBS-EP+). Within a single binding cycle, samples of C-CPE or its derivatives were injected sequentially in order of increasing concentration over both the ligand and the reference surfaces. The reference surface, an unmodified flowcell, was used to correct for systematic noise and instrumental drift. Also, prior to the binding cycle for C-CPE or its derivatives, buffer was injected. These "blank" responses were used as a double-reference for the binding data [28]. The sensorgrams were globally fitted by using a 1:1 binding model to determine k_a, k_d and K_D values with the Biacore T100 Evaluation Software version 2.0.1.

2.7. Transepithelial electric resistance (TEER) assay

Caco-2 cells were seeded onto BD BioCoat™ Fibrillar Collagen Cell culture inserts (BD Biosciences, San Jose, CA) at a density of 1×10^5 cells/insert and cultured for 5 days. TJ barriers were formed by a 3-day culture in Entero-STIM™ (BD Biosciences) medium for cellular differentiation. C-CPE or its derivatives were added to the apical side of the chamber. After 18 h of incubation, the TEER values were measured with a Millicell-ERS epithelial volt-ohmmeter (Millipore, Billerica, MA). The percentage changes of TEER values were calculated by the ratio to TEER value in 100 μg/ml of C-CPE184. EC50 values, at which the TEER ratio is 50%, were calculated by using the four-parameter logistic function of DeltaSoft version 3 (BioMetallics, Princeton, NJ) from dose–response curves of the TEER ratio.

2.8. In situ loop assay

Jejunal absorption of hPTH(1-34) or fluorescein isothiocyanate-dextran with a molecular mass of 4 kDa (FD-4) was evaluated by using an in situ loop assay as described previously [21]. The experiments were performed according to the guidelines of the ethics committee of Osaka University or Asubio Pharma Co. Ltd. After 7-week-old Wister male rats were anesthetized with pentobarbital, a midline abdominal incision was made, and the jejunum was washed with PBS. A 5-cm long jejunal loop was prepared by closing both ends with sutures. hPTH(1-34) (100 μg) was co-administered with C-CPEs into the loop or administered 4 h after the administration of C-CPEs. Blood was collected from the femoral artery by using a cannulated polyethylene tube at the indicated time points. EDTA (1 mg/ml) was immediately added to the blood sample, and the plasma was recovered by centrifugation. To avoid degradation of hPTH(1-34), aprotinin (500 IU/ml) was immediately added to the plasma, and the plasma was stored at −80 °C until use. The plasma hPTH(1-34) was quantified by radioimmunoassay (RIA) with anti-hPTH antibody. Anti-hPTH antibody was added to the plasma and then incubated with [^{125}I-Tyr34] hPTH(1-34) (15,000–20,000 cpm/100 μl) for 24 h. The anti-rabbit IgG goat antibody was added, and anti-hPTH antibody bound to the anti-rabbit IgG goat antibody was separated by centrifugation. The radioactivity in the sediment was counted with a gamma counter (PerkinElmer Inc., Waltham, MA). The area under the plasma concentration time curve (AUC) from 0 to 120 min after administration was calculated by the trapezoidal method. Relative bioavailability (BA) was calculated with the following equation: BA (%) = (AUC (ng·min/ml)/dose (μg/kg))/(AUC (iv)(ng·min/ml)/dose (iv) (μg/kg)). AUC (iv) indicates the $AUC_{0-120\ min}$ of intravenously administered hPTH(1-34) (10 μg/kg), and the AUC value is 208.6 ± 52.7 ng·min/ml.

Rats were anesthetized with thiamylal sodium, and a jejunal loop was made, as described above. A mixture of FD-4 (2 mg) and C-CPEs was co-administered into the jejunal loop. Blood was collected from the jugular vein at the indicated time points. The plasma levels of FD-4 were measured with a fluorescence spectrophotometer (Fluoroskan Ascent FL; ThermoElectron Corporation, Waltham, MA). The AUC of FD-4 from 0 to 6 h ($AUC_{0-6\ h}$) was calculated by the trapezoidal method.

2.9. Nasal and pulmonary absorption assay

Nasal and pulmonary absorption of hPTH(1-34) was examined in 7-week-old Sprague–Dawley male rats. The experiments were performed according to the guidelines of the ethics committee of Asubio Pharma Co. Ltd. For the nasal absorption assay, 200 μg of hPTH(1-34) was intranasally administered to both sides of the nasal cavity 0 or 4 h after nasal administration of C-CPEs. The total injection volume did not exceed 20 μl. For the pulmonary absorption assay, a polyethylene tube (PE-240, Clay Adams, Becton Dickinson & Co., Sparks, MD) was inserted into the trachea of each rat. A MicroSprayer (Penn-Century, Inc., Philadelphia, PA) was used to perform pulmonary injections of C-CPEs; then, after 0 or 4 h, 150 μg of hPTH(1-34) was administered with the MicroSprayer. Blood was collected at the indicated time points, and the plasma concentration of hPTH(1-34) was measured by RIA, as described above. AUC and BA (%) values were calculated, as described above.

2.10. Statistical analysis

Data were analyzed by using analysis of variance (ANOVA) followed by Dunnett's multiple comparison test, and statistical significance was assigned at $p < 0.05$.

3. Results

3.1. Effects of C-CPE on jejunal, nasal and pulmonary absorption of a peptide drug

We previously found that a claudin-4 modulator, C-CPE184, is a novel type of absorption enhancer by using dextran as a model drug [21]. In the present study, we investigated whether the claudin-4 modulator enhances jejunal, nasal and pulmonary absorption of a peptide drug, hPTH(1-34). When hPTH(1-34) was administered with C-CPE184, C-CPE184 enhanced nasal absorption of hPTH(1-34) by 2.5-fold as compared to the vehicle-treated group. However, C-CPE184 did not enhance jejunal and pulmonary absorption of hPTH(1-34) (Fig. 1 and Table 1). Next, we examined whether pre-treatment of mucosa with C-CPE184 enhanced absorption of hPTH(1-34). When hPTH(1-34) was administered after 4 h of treatment with C-CPE184, the jejunal, nasal and pulmonary absorption of hPTH(1-34) was significantly

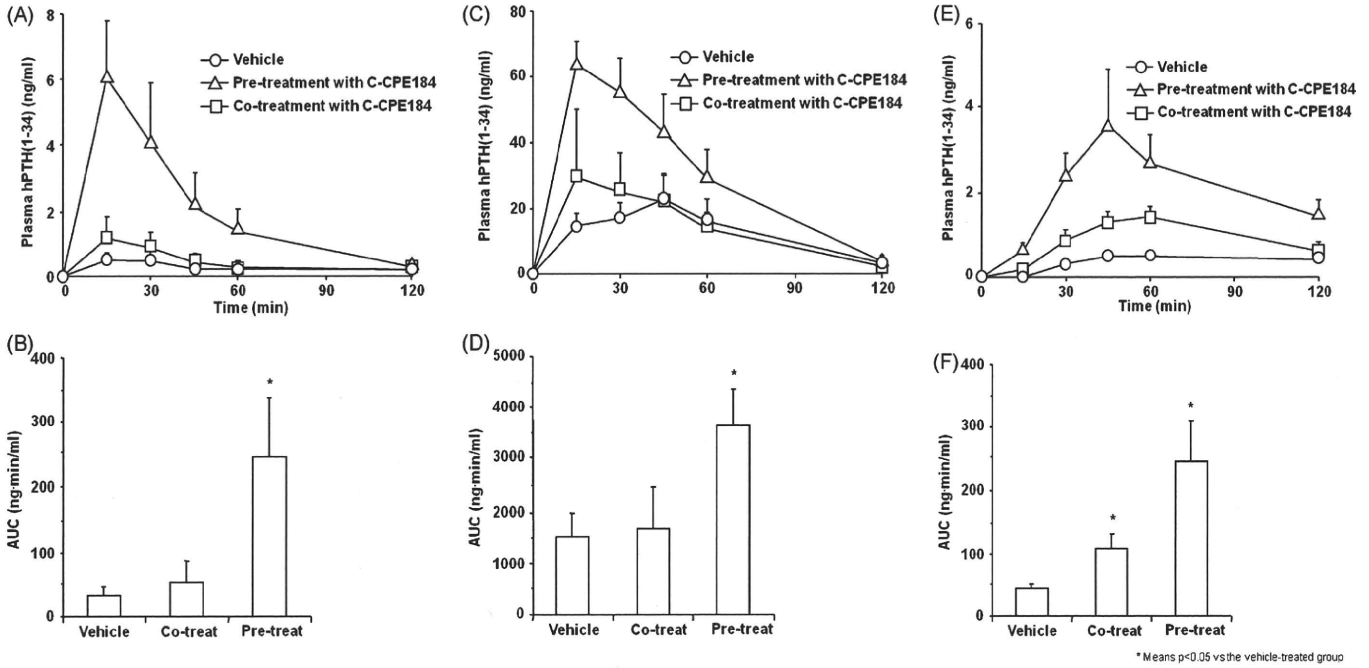

Fig. 1. Effect of C-CPE184 on mucosal absorption of hPTH(1-34) in rats. (A, B) Jejunal absorption of hPTH(1-34). Jejunum was co-treated with hPTH(1-34) (100 μg) and C-CPE184 (20 μg), or jejunum was treated with hPTH(1-34) 4 h after treatment with C-CPE184. (C, D) Pulmonary absorption of hPTH(1-34). hPTH(1-34) (150 μg) was pulmonary administered with C-CPE184 (5 μg) or 4 h after administration of C-CPE184. (E, F) Nasal absorption of hPTH(1-34). hPTH(1-34) (200 μg) was nasally administered with C-CPE184 (2 μg) or 4 h after administration of C-CPE184. Plasma hPTH(1-34) levels were measured at the indicated periods. Time-course changes in plasma hPTH(1-34) levels (A, C, E) and AUC from 0 to 120 min (B, D, F) were calculated. Data are mean ± SE (n = 3-6). Co-treat indicates co-treatment with both hPTH and C-CPE184, and Pre-treat indicates treatment with hPTH 4 h after C-CPE184-treatment. *Significantly different from the vehicle-treated group ($p < 0.05$).

Table 1
Parameters of mucosal absorption of hPTH(1-34) in C-CPE184-treated rats.

Treatments	Jejunum		Nasal		Pulmonary	
	Cmax (ng/ml)	BA (%)[a]	Cmax (ng ml)	BA (%)	Cmax (ng ml)	BA (%)
Vehicle	0.9 ± 0.3	0.4 ± 0.2	0.7 ± 0.1	0.3 ± 0.0	27.8 ± 6.5	14.6 ± 4.4
Co-treat	1.2 ± 0.6	0.6 ± 0.4	1.5 ± 0.2*	0.8 ± 0.2*	35.2 ± 18.9	14.9 ± 6.5
Pre-treat	6.0 ± 1.8*	2.7 ± 0.9*	3.6 ± 1.3	1.4 ± 0.4*	67.6 ± 7.5**	34.5 ± 6.6*

[a] BA (%) = (AUC/Dose)/(AUC iv/Dose iv).
Data are means ± SE.
*$p < 0.05$, **$p < 0.01$, as compared to vehicle-treated group.

increased 7.5-, 5.6- and 2.4-fold compared to the vehicle-treated group (Fig. 1 and Table 1).

3.2. Preparation of N-terminal-truncated C-CPE184-319 derivatives

The solubility of C-CPE184 is less than 0.3 mg/ml in PBS due to its hydrophobicity (Table 2). An increase in solubility without loss of claudin-4-modulating activity might improve the mucosal-absorption-enhancing activity of C-CPE184. Van Itallie et al. showed that the removal of the 10 N-terminal amino acids from C-CPE184 to yield C-CPE194 results in high solubility (10 mg/ml)

Table 2
Solubility of C-CPE184 and the N-terminal-truncated mutants.

Derivatives	Molecular size (kDa)	Solubility[a] (mg/ml)
C-CPE184	18.2	<0.3
C-CPE194	17.3	>10
C-CPE205	16.1	>4
C-CPE212	15.4	Insol.[b]
C-CPE219	14.7	Insol.
C-CPE224	14.2	Insol.

[a] Solvent is PBS.
[b] Insol., insoluble.

[26]. Although C-CPE194 is a claudin-4 binder, whether C-CPE194 modulates the TJ-barrier remains unclear. C-CPE194 contains nine β-sheets and one α-helix, and its 16 C-terminal amino acids are believed to comprise the claudin-4-binding region (Fig. 2A) [26,29]. Based on this information, we prepared five different N-terminal-truncated C-CPE184 derivatives: C-CPE194, which lacks the 10 N-terminal amino acids; C-CPE205, which is truncated prior to the β1-sheet; C-CPE212, which is truncated after the β1-sheet; C-CPE219, which is truncated after the α-helix; and C-CPE224, which is truncated before the β2-sheet (Fig. 2A). The C-CPEs were expressed in *E. coli* (Fig. 2B). The solubility of C-CPE194 (>10 mg/ml) and C-CPE205 (>4 mg/ml) in PBS was greater than that of C-CPE184 (<0.3 mg/ml) (Table 2). However, C-CPE212, C-CPE219 and C-CPE224 formed solid inclusion bodies in *E. coli*, and these inclusion bodies could not be dissolved without 2 M urea. Therefore, further experiments were performed with C-CPE184, C-CPE194 and C-CPE205.

3.3. Characterization of C-CPE194 and C-CPE205

To study the interaction between the C-CPEs and claudin-4, we performed ELISA with claudin-4-displaying BV, as described previously [24]. When C-CPEs were added to claudin-4-displaying

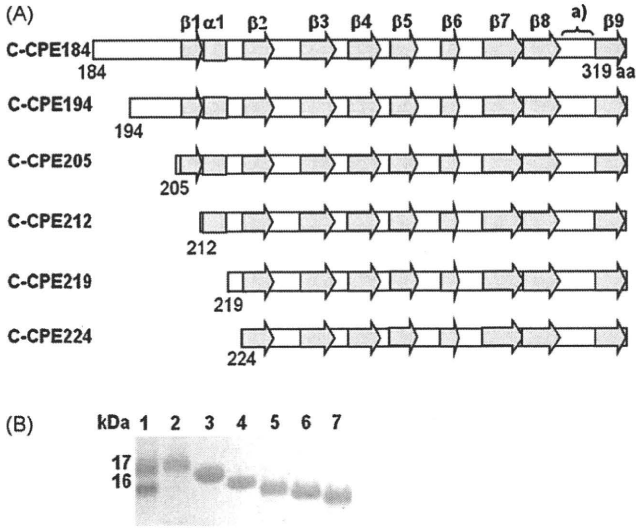

Fig. 2. Preparation of C-CPEs. (A) Schematic structure of C-CPEs. Van Itallie et al. determined the 3-dimensional structure of C-CPE194 containing nine β-sheets and one α-helix [26]. Based on the structural information, we designed five N-terminal truncated C-CPE184 derivatives. (B) CBB staining. C-CPEs were prepared and then purified by affinity chromatography. Lane 1, a maker for molecular weight; lane 2, C-CPE184; lane 3, C-CPE194; lane 4, C-CPE205; lane 5, C-CPE212; lane 6, C-CPE219; lane 7, C-CPE224.

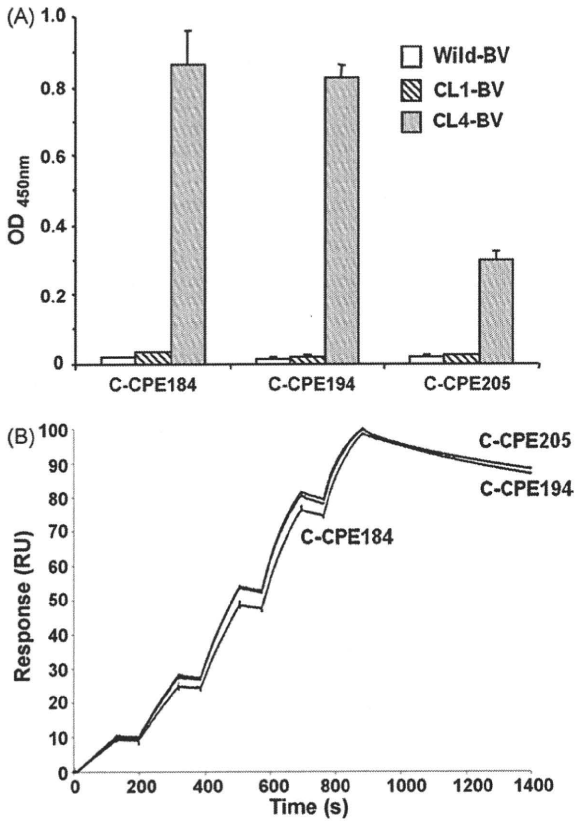

Fig. 3. Interaction of C-CPEs with claudin. (A) ELISA. The immunoplate was coated with wild-type BV (Wild-BV), claudin-1-displaying BV (CL1-BV) or claudin-4-displaying BV (CL4-BV), and then C-CPEs were added to the well. C-CPEs bound to BVs were detected by the addition of anti-his tag antibody and a labeled secondary antibody. Data are means ± SD (n = 3). (B) SPR assay. Claudin-4 was immobilized on a CM5 sensor chip by the amine-coupling method. C-CPEs were injected sequentially at concentrations of 1.25, 2.5, 5, 10 and 20 nM. The association phase was monitored for 120 s at a flow rate of 10 μl/min, and the dissociation phase was followed for 600 s at the same flow rate. The maximum values of response (Rmax) for all curves were compensated to 100 RU.

Table 3
Binding kinetics of C-CPEs to claudin-4.

Derivatives	k_a (1/Ms)	k_d (1/s)	K_D
C-CPE184	5.96×10^5	2.55×10^{-4}	429 pM
C-CPE194	7.13×10^5	3.24×10^{-4}	455 pM
C-CPE205	7.67×10^5	2.87×10^{-4}	374 pM

BV-adsorbed immunoplates, C-CPE194 and C-CPE205 bound to claudin-4-displaying BV but not mock BV or claudin-1-displaying BV (Fig. 3A). We performed SPR analysis to compare the affinities of C-CPEs to claudin-4. Claudin-4 proteins were fixed on the sensor chip, and C-CPEs were injected. Then, we measured the interaction between claudin-4 and C-CPEs. As shown in Fig. 3B and Table 3, C-CPE184, C-CPE194 and C-CPE205 had almost the same affinity to claudin-4 with K_D values of 429, 455 and 374 pM, respectively. The association and dissociation rates of C-CPE194 and C-CPE205 were also similar to those of C-CPE184. C-CPE184, C-CPE194 and C-CPE205 showed similar TJ-modulating activities in Caco-2 monolayer cells; their EC50 values were 0.49, 0.57 and 0.51 μg/ml, respectively (Fig. 4A and Table 4). We performed in situ loop assays to examine the jejunal absorption of FD-4 by C-CPEs. C-CPE194 and C-CPE205 enhanced the jejunal absorption of FD-4 similar to C-CPE184 at 0.2 mg/ml (Fig. 4B–D). Treatment with C-CPE194 or C-CPE205 at 1.0 mg/ml yielded a greater and earlier absorption of FD-4 than treatment at 0.2 mg/ml (Fig. 4B, C). We could not test 1.0 mg/ml of C-CPE184 due to its low solubility.

3.4. Jejunal and pulmonary absorption of hPTH(1-34) by co-treatment with C-CPE194

C-CPE194 enhanced the jejunal absorption of FD-4 to a similar extent as C-CPE184 and C-CPE205; C-CPE194 was also 30- and 3-fold more soluble than C-CPE184 and C-CPE205, respectively. C-CPE194 enhanced the jejunal absorption of hPTH(1-34) at 0.2 and 4.0 mg/ml (Fig. 5A). The AUC values were increased 11.0- and 18.4-fold as compared to the vehicle-treated group (Fig. 5B), and the Cmax and BA of the jejunal absorption of hPTH(1-34) were also increased by C-CPE194 (Table 5). Additionally, the pulmonary absorption of hPTH(1-34) was enhanced by C-CPE194 (AUC = 3080.0 ± 1994.3 ng·min/ml in vechicle-treated group, AUC = 13,397.7 ± 5830.1 ng·min/ml in C-CPE194 (0.8 mg/ml)-treated group) (Fig. 5C, D). The Cmax and BA of hPTH(1-34) were also increased by C-CPE194 (Table 5).

4. Discussion

Biologics are generally hydrophilic and poorly absorbed by the mucosa; therefore, many biologics are administered via injection. The development of a delivery system to allow biologics to pass across the epithelial barrier in mucosa is a pivotal issue for pharmaceutical therapy with biologics, since mucosal administration is needle-free, non-invasive, convenient and comfortable for patients [30,31]. We previously found that C-CPE184 enhanced jejunal absorption of dextran with a molecular mass of <10 kDa through its modulation of the claudin-4 barrier [21]. In the present study, we investigated the effect of a claudin-4 modulator on the mucosal absorption of a biologic, hPTH(1-34), and we found that a claudin-4 modulator is also a potent jejunal, nasal and pulmonary absorption enhancer of this biologic.

CPE is a 35-kDa polypeptide consisting of 319 amino acids [32]. The functional domain of CPE is divided into an N-terminal toxic domain and a C-terminal receptor-binding domain [33]. The receptor-binding fragments of CPE correspond to amino acids 169–319, 171–319, 184–319, 194–319 and 290–319 [20,26,33–35]. Among these fragments, only C-CPE184 and C-CPE194 have been

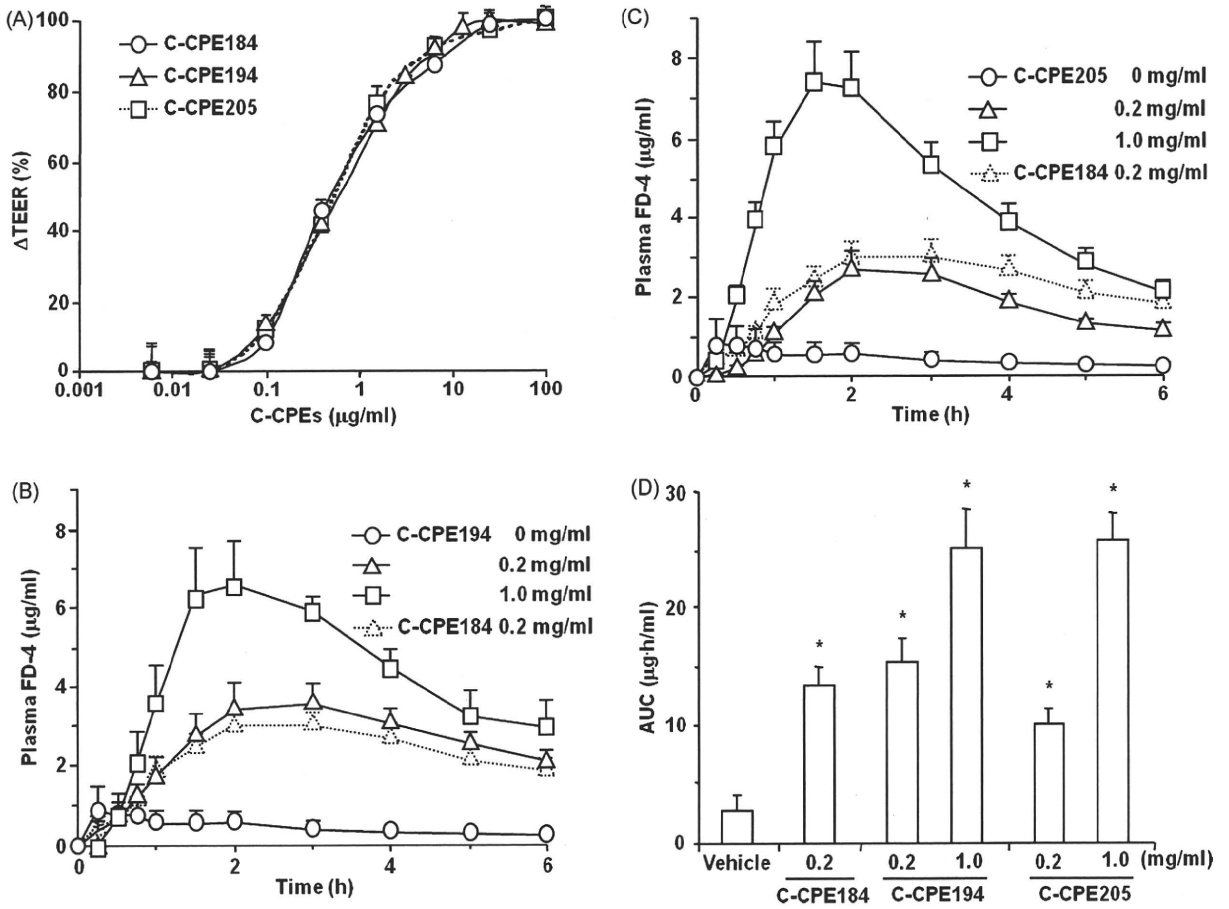

Fig. 4. Modulation of the TJ-barrier by C-CPEs. (A) Caco-2 cells were seeded on a BioCoat™. When TJ-barriers were developed and the cell sheets reached a plateau in their TEER value, C-CPEs were added to the wells from the basal side at the indicated concentration. After 18 h, the TEER was measured. The ΔTEER was calculated as the ratio to reduced TEER values at 0 and 100 μg/ml of C-CPE184 as 0% and 100%, respectively. Data are mean ± SD ($n = 3$). (B–D) Jejunal absorption of FD-4. Jejunum were treated with FD-4 and C-CPEs at the indicated concentration. Time-course changes in plasma FD-4 levels (B, C) and AUC from 0 to 6 h (D). Data are means ± SE ($n = 4$–9). *Significantly different from the vehicle-treated group ($p < 0.05$).

proven to bind to claudin-4 [10,26], and a mucosal-absorption-enhancing effect was proven only for C-CPE184 [21]. The claudin-4 modulator C-CPE184 is a 400-fold more potent jejunal absorption enhancer of dextran as compared to a clinically used absorption enhancer, sodium caprate [21]. However, the low solubility of C-CPE184 (<0.3 mg/ml in PBS) has limited its applicability. This low solubility may result in the slow onset of TJ opening due to limiting the access of C-CPE184 to claudin. Last year, Van Itallie et al. made a breakthrough by truncating the N-terminal of C-CPE184 by 10 amino acids to yield C-CPE194 [26]. They found that C-CPE194 has affinity to claudin-4 and high solubility (>10 mg/ml); moreover, they determined the 3-dimensional structure of C-CPE194, which contains nine β-sheets and one α-helix, and they suggested that the intervening surface loop spanning region 304–312 (located between the β8 and β9 sheets) may be a claudin-binding domain. Based on the structural data for C-CPE194, we prepared five N-terminal-truncated C-CPE184 derivatives: C-CPE194, C-CPE205, C-CPE212 (without the β1 sheet), C-CPE219 (without the β1 sheet and α helix), and C-CPE224 (without the β1 sheet and α helix). C-CPEs lacking the β1 sheet are soluble in PBS containing 2 M Urea but insoluble in PBS. C-CPE184, C-CPE194 and C-CPE205 have almost the same kinetics parameters for binding to claudin-4 and the same TJ-barrier modulating activity (Table 3, Fig. 4A). Thus, the β1 sheet appears to be critical for maintaining the structure of C-CPE, and the N-terminal region corresponding to amino acids 184–204 may not be involved in claudin-4 binding or TJ-barrier modulation.

Table 4
TJ-modulating activities of C-CPEs in Caco-2 cells.

Derivatives	EC50 values[a]
C-CPE184	0.49 μg/ml
C-CPE194	0.57 μg/ml
C-CPE205	0.51 μg/ml

[a] The concentration of C-CPEs at which a 50% decrease in TEER value was observed in Fig. 4A.

Biologics must escape degradation by mucosal enzymes to be absorbed by the mucosa. C-CPE184 (0.2 mg/ml) did not enhance jejunal or pulmonary absorption of hPTH(1-34). However, when hPTH(1-34) was administered 4 h after treatment with C-CPE184, jejunal, pulmonary and nasal absorption was enhanced. Thus, hPTH(1-34) may be degraded in the jejunal and pulmonary mucosa before the enhancement of its absorption by co-administered C-CPE184. Indeed, another claudin-4 modulator, C-CPE194, which is 30-fold more soluble than C-CPE184, significantly enhanced the jejunal and pulmonary absorption of hPTH(1-34). These findings indicate that modulation of claudin-4 may be a potent strategy for mucosal-absorption enhancement of biologics.

Meanwhile, a critical issue in the clinical application of the claudin-4 modulator as a mucosal-absorption enhancer is its safety. Problems with the safety of a claudin-4 modulator include the safety of a claudin-4 modulator in itself and the safety of the modulation of claudin-4, i.e., entry of unwanted substances by the

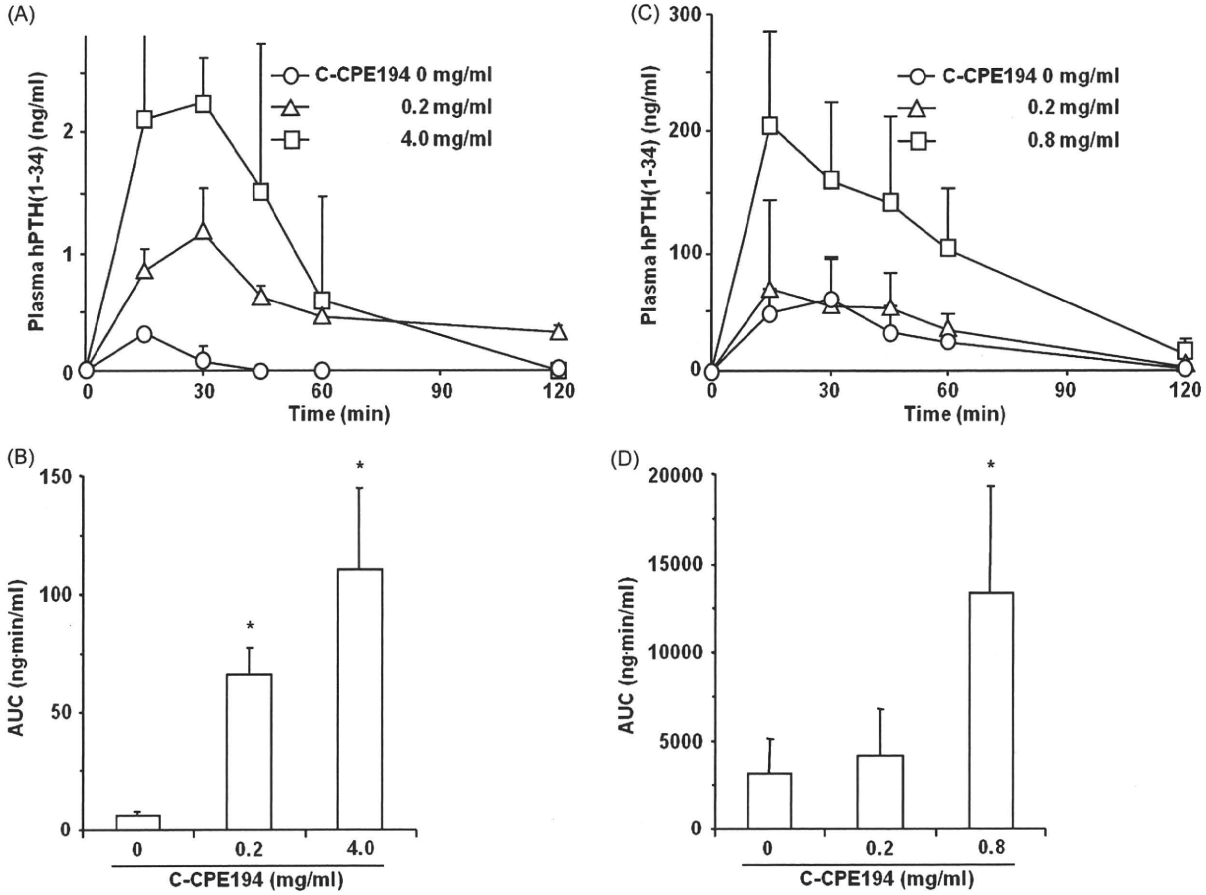

Fig. 5. Mucosal absorption of hPTH(1-34) by a claudin-4 modulator. (A, B) Jejunal absorption of hPTH(1-34). Rat jejunum was treated with hPTH(1-34) (100 μg) and C-CPE194 at the indicated doses. Time-course changes in plasma hPTH(1-34) (A) and AUC from 0 to 120 min (B) were analyzed. (C, D) Pulmonary absorption of hPTH(1-34). hPTH(1-34) (150 μg) and C-CPE194 at the indicated doses were pulmonary administered, and time-course changes in plasma hPTH(1-34) concentration (C) and AUC from 0 to 120 min (D) were analyzed. Data are mean ± SE ($n = 3$). *Significantly different from the vehicle-treated group ($p < 0.05$).

opening of TJs. As mentioned above, C-CPEs are the only claudin-4 modulator. C-CPEs are polypeptide fragments of CPE consisting of more than 120 amino acids, and C-CPEs themselves may have antigenicity. Claudin-4 modulator significantly enhanced jejunal absorption of dextran with a molecular mass of less than 10 kDa [21], and C-CPEs (>14.2 kDa) may not be absorbed by the modulation of claudin-4. Moreover, *C. perfringens* are indigenous bacterium, and immunological tolerance may be induced. Thus, the antigenicity of C-CPE might be partly negligible. Because absorption enhancers would be used as an additive in drugs, they would be repeatedly administered. To avoid the risk of antigenicity, the development of a chemical compound-type or a 30–40 mer peptide-type of claudin modulator is needed. The determination of the 3-dimensional structure of claudin is also important for the theoretical development of promising claudin modulators. Ling et al. prepared a 12-mer peptide-type claudin-4 binder which did not modulate TJs [36], and Van Itallie et al. determined the structure of C-CPE [26]. A peptide-type claudin modulator will be developed in the near future.

The other safety issue is the possible influx of unwanted substances that could be caused by the opening of TJs. C-CPE has demonstrated no damages to mucosal epithelial tissue in rat intestine [21]. Treatment of cells with C-CPE decreased the level of intracellular claudin-4 proteins paralleled by a disruption of the TJ-barrier [10]. Claudin contains the clathrin-sorting signal in its C-terminal intracellular domain, and claudin was often internalized [37,38]. Taken together, these results indicate that C-CPEs may disrupt the TJ-barrier, allowing the movement of solutes through the paracellular route. Do claudin modulators reversibly modulate the TJ-barrier and specifically regulate the movement of solutes? Disruption of the TJ-barrier by C-CPE is reversible, and the TJ-barrier gradually recovered after the removal of C-CPE [10]. The

Table 5
Parameters of mucosal absorption of hPTH(I-34) in C-CPE 194-treated rats.

C-CPE194 (mg/ml)	Jejunum		C-CPE194 (mg/ml)	Pulmonary	
	Cmax (ng/ml)	BA (%)[a]		Cmax (ng/ml)	BA (%)
0	0.3 ± 0.0	0.1 ± 0.0	0	62.3 ± 32.8	26.5 ± 17.4
0.2	1.2 ± 0.4*	0.8 ± 0.2**	0.2	78.7 ± 66.1	34.1 ± 21.6
4.0	2.8 ± 0.2*	1.3 ± 0.3**	0.8	205.2 ± 79.4*	100.6 ± 39.3*

[a] BA (%) = (AUC/Dose)/(AUC iv/Dose iv).
Data are mean ± SE.
*$p < 0.05$, **$p < 0.01$ as compared to the vehicle-treated group.

quick recovery of TJ-barriers will need to be facilitated. One approach is the development of a quickly reversible claudin modulator. Another approach is the development of a claudin inducer for the combination of a claudin modulator and inducer. Another approach is the reduction of unwanted transport using the properties of claudins. Claudin comprises a multigene family consisting of 24 members. Claudin forms paired TJ strands by polymerization in a homomeric and heteromeric manner, and the claudin strands interact in a homotypic and heterotypic manner between adjacent cells [39,40]. TJ-barrier properties are believed to be determined by the combination and mixing ratios of claudin species [41]. Interestingly, the diversity of claudin may contribute to the regulation of specific solute movement through the paracellular route [17]. The expression profiles of claudin in mucosal epithelium exhibit heterogeneity [13–15,42]. The development of claudin modulators with solute and tissue specificity will reduce the non-specific influx of solutes caused by the modulation of TJs.

In summary, we found that claudin-4 modulator enhanced the jejunal, pulmonary and nasal absorption of a peptide drug. This report is the first to indicate that a claudin-4 modulator may be a mucosal-absorption enhancer of biologics.

Acknowledgments

We thank M. Hoshino (Asubio Pharma), N. Kumagai (Asubio Pharma), K. Takashiba (Asubio Pharma), R. Okude (Osaka University) and Y. Nakano (GE Healthcare, Japan) for their excellent technical assistance. We also thank Drs Y. Horiguchi (Osaka University) and M. Furuse (Kobe University) for providing us C-CPE cDNA and claudin cDNA, respectively. This work was supported by a Grant-in-Aid for Scientific Research (21689006) from the Ministry of Education, Culture, Sports, Science and Technology, Japan, by a Health and Labor Sciences Research Grants from the Ministry of Health, Labor and Welfare of Japan and by a grant from Kansai Biomedical Cluster project in Saito, which is promoted by the Knowledge Cluster Initiative of the Ministry of Education, Culture, Sports, Science and Technology, Japan.

References

[1] Powell DW. Barrier function of epithelia. Am J Physiol 1981;241:G275–88.
[2] Engel RH, Riggi SJ. Effect of sulfated and sulfonated surfactants on the intestinal absorption of heparin. Proc Soc Exp Biol Med 1969;130:879–84.
[3] Tidball CS, Lipman RI. Enhancement of jejunal absorption of heparinoid by sodium ethylenediaminetetraacetate in the dog. Proc Soc Exp Biol Med 1962;111:713–5.
[4] Aungst BJ. Intestinal permeation enhancers. J Pharm Sci 2000;89:429–42.
[5] Deli MA. Potential use of tight junction modulators to reversibly open membranous barriers and improve drug delivery. Biochim Biophys Acta 2009;1788:892–910.
[6] Matsuhisa K, Kondoh M, Takahashi A, Yagi K. Tight junction modulator and drug delivery. Expert Opin Drug Deliv 2009;6:509–15.
[7] Kondoh M, Yoshida T, Kakutani H, Yagi K. Targeting tight junction proteins-significance for drug development. Drug Discov Today 2008;13:180–6.
[8] Furuse M, Hirase T, Itoh M, Nagafuchi A, Yonemura S, Tsukita S, et al. Occludin: a novel integral membrane protein localizing at tight junctions. J Cell Biol 1993;123:1777–88.
[9] Furuse M, Fujita K, Hiiragi T, Fujimoto K, Tsukita S. Claudin-1 and -2: novel integral membrane proteins localizing at tight junctions with no sequence similarity to occludin. J Cell Biol 1998;141:1539–50.
[10] Sonoda N, Furuse M, Sasaki H, Yonemura S, Katahira J, Horiguchi Y, et al. *Clostridium perfringens* enterotoxin fragment removes specific claudins from tight junction strands: evidence for direct involvement of claudins in tight junction barrier. J Cell Biol 1999;147:195–204.
[11] Furuse M, Hata M, Furuse K, Yoshida Y, Haratake A, Sugitani Y, et al. Claudin-based tight junctions are crucial for the mammalian epidermal barrier: a lesson from claudin-1-deficient mice. J Cell Biol 2002;156:1099–111.
[12] Nitta T, Hata M, Gotoh S, Seo Y, Sasaki H, Hashimoto N, et al. Size-selective loosening of the blood-brain barrier in claudin-5-deficient mice. J Cell Biol 2003;161:653–60.
[13] Rahner C, Mitic LL, Anderson JM. Heterogeneity in expression and subcellular localization of claudins 2, 3, 4, and 5 in the rat liver, pancreas, and gut. Gastroenterology 2001;120:411–22.
[14] Takano K, Kojima T, Go M, Murata M, Ichimiya S, Himi T, et al. HLA-DR- and CD11c-positive dendritic cells penetrate beyond well-developed epithelial tight junctions in human nasal mucosa of allergic rhinitis. J Histochem Cytochem 2005;53:611–9.
[15] Wang F, Daugherty B, Keise LL, Wei Z, Foley JP, Savani RC, et al. Heterogeneity of claudin expression by alveolar epithelial cells. Am J Respir Cell Mol Biol 2003;29:62–70.
[16] Krause G, Winkler L, Mueller SL, Haseloff RF, Piontek J, Blasig IE. Structure and function of claudins. Biochim Biophys Acta 2008;1778:631–45.
[17] Krause G, Winkler L, Piehl C, Blasig I, Piontek J, Muller SL. Structure and function of extracellular claudin domains. Ann N Y Acad Sci 2009;1165:34–43.
[18] McClane BA, Hanna PC, Wnek AP. *Clostridium perfringens* enterotoxin. Microb Pathog 1988;4:317–23.
[19] Fujita K, Katahira J, Horiguchi Y, Sonoda N, Furuse M, Tsukita S. *Clostridium perfringens* enterotoxin binds to the second extracellular loop of claudin-3, a tight junction integral membrane protein. FEBS Lett 2000;476:258–61.
[20] Katahira J, Inoue N, Horiguchi Y, Matsuda M, Sugimoto N. Molecular cloning and functional characterization of the receptor for *Clostridium perfringens* enterotoxin. J Cell Biol 1997;136:1239–47.
[21] Kondoh M, Masuyama A, Takahashi A, Asano N, Mizuguchi H, Koizumi N, et al. A novel strategy for the enhancement of drug absorption using a claudin modulator. Mol Pharmacol 2005;67:749–56.
[22] Wray C, Mao Y, Pan J, Chandrasena A, Piasta F, Frank JA. Claudin-4 augments alveolar epithelial barrier function and is induced in acute lung injury. Am J Physiol Lung Cell Mol Physiol 2009;297:L219–27.
[23] Suzuki Y, Yabuta M, Ohsuye K. High-level production of recombinant human parathyroid hormone 1-34. Appl Environ Microbiol 1998;64:526–9.
[24] Saeki R, Kondoh M, Kakutani H, Tsunoda SI, Mochizuki Y, Hamakubo T, et al. A novel tumor-targeted therapy using a claudin-4-targeting molecule. Mol Pharmacol 2009;76:918–26.
[25] Mitic LL, Unger VM, Anderson JM. Expression, solubilization, and biochemical characterization of the tight junction transmembrane protein claudin-4. Protein Sci 2003;12:218–27.
[26] Van Itallie CM, Betts L, Smedley 3rd JG, McClane BA, Anderson JM. Structure of the claudin-binding domain of *Clostridium perfringens* enterotoxin. J Biol Chem 2008;283:268–74.
[27] Karlsson R, Katsamba PS, Nordin H, Pol E, Myszka DG. Analyzing a kinetic titration series using affinity biosensors. Anal Biochem 2006;349:136–47.
[28] Myszka DG. Improving biosensor analysis. J Mol Recognit 1999;12:279–84.
[29] Takahashi A, Komiya E, Kakutani H, Yoshida T, Fujii M, Horiguchi Y, et al. Domain mapping of a claudin-4 modulator, the C-terminal region of C-terminal fragment of *Clostridium perfringens* enterotoxin, by site-directed mutagenesis. Biochem Pharmacol 2008;75:1639–48.
[30] Sayani AP, Chien YW. Systemic delivery of peptides and proteins across absorptive mucosae. Crit Rev Ther Drug Carrier Syst 1996;13:85–184.
[31] Song Y, Wang Y, Thakur R, Meidan VM, Michniak B. Mucosal drug delivery: membranes, methodologies, and applications. Crit Rev Ther Drug Carrier Syst 2004;21:195–256.
[32] Czeczulin JR, Hanna PC, McClane BA. Cloning, nucleotide sequencing, and expression of the *Clostridium perfringens* enterotoxin gene in *Escherichia coli*. Infect Immun 1993;61:3429–39.
[33] Hanna PC, Wieckowski EU, Mietzner TA, McClane BA. Mapping of functional regions of *Clostridium perfringens* type A enterotoxin. Infect Immun 1992;60:2110–4.
[34] Hanna PC, Mietzner TA, Schoolnik GK, McClane BA. Localization of the receptor-binding region of *Clostridium perfringens* enterotoxin utilizing cloned toxin fragments and synthetic peptides. The 30 C-terminal amino acids define a functional binding region. J Biol Chem 1991;266:11037–43.
[35] Kokai-Kun JF, McClane BA. Deletion analysis of the *Clostridium perfringens* enterotoxin. Infect Immun 1997;65:1014–22.
[36] Ling J, Liao H, Clark R, Wong MS, Lo DD. Structural constraints for the binding of short peptides to claudin-4 revealed by surface plasmon resonance. J Biol Chem 2008;283:30585–9.
[37] Ivanov AI, Nusrat A, Parkos CA. Endocytosis of epithelial apical junctional proteins by a clathrin-mediated pathway into a unique storage compartment. Mol Biol Cell 2004;15:176–88.
[38] Matsuda M, Kubo A, Furuse M, Tsukita S. A peculiar internalization of claudins, tight junction-specific adhesion molecules, during the intercellular movement of epithelial cells. J Cell Sci 2004;117:1247–57.
[39] Furuse M, Furuse K, Sasaki H, Tsukita S. Conversion of zonulae occludentes from tight to leaky strand type by introducing claudin-2 into Madin-Darby canine kidney I cells. J Cell Biol 2001;153:263–72.
[40] Furuse M, Sasaki H, Tsukita S. Manner of interaction of heterogeneous claudin species within and between tight junction strands. J Cell Biol 1999;147:891–903.
[41] Furuse M, Tsukita S. Claudins in occluding junctions of humans and flies. Trends Cell Biol 2006;16:181–8.
[42] Coyne CB, Gambling TM, Boucher RC, Carson JL, Johnson LG. Role of claudin interactions in airway tight junctional permeability. Am J Physiol Lung Cell Mol Physiol 2003;285:L1166–78.

Journal of Controlled Release 142 (2010) 431–437

Contents lists available at ScienceDirect

Journal of Controlled Release

journal homepage: www.elsevier.com/locate/jconrel

Prevention of hepatic ischemia–reperfusion injury by pre-administration of catalase-expressing adenovirus vectors

Masahiro Ushitora [a,b], Fuminori Sakurai [a,*], Tomoko Yamaguchi [a,c], Shin-ichiro Nakamura [d], Masuo Kondoh [b], Kiyohito Yagi [b], Kenji Kawabata [a], Hiroyuki Mizuguchi [a,c,*]

[a] Laboratory of Gene Transfer and Regulation, National Institute of Biomedical Innovation, Osaka, Japan
[b] Laboratory of Bio-Functional Molecular Chemistry, Graduate School of Pharmaceutical Sciences, Osaka University, Osaka, Japan
[c] Department of Biochemistry and Molecular Biology, Graduate School of Pharmaceutical Sciences, Osaka University, Osaka, Japan
[d] Research Center of Animal Life Science, Shiga University of Medical Science, Otsu-City, Shiga, Japan

ARTICLE INFO

Article history:
Received 17 August 2009
Accepted 25 November 2009
Available online 29 November 2009

Keywords:
Adenovirus vector
Reactive oxygen
Ischemia/reperfusion
Liver
Catalase
Hepatectomy

ABSTRACT

Liver ischemia/reperfusion (I/R) injury, which is mainly caused by the generation of reactive oxygen species (ROS) during the reperfusion, remains an important clinical problem associated with liver transplantation and major liver surgery. Therefore, ROS should be detoxified to prevent hepatic I/R-induced injury. Delivery of antioxidant genes into liver is considered to be promising for prevention of hepatic I/R injury; however, therapeutic effects of antioxidant gene transfer to the liver have not been fully examined. The aim of this study was to examine whether adenovirus (Ad) vector-mediated catalase gene transfer in the liver is an effective approach for scavenging ROS and preventing hepatic I/R injury. Intravenous administration of Ad vectors expressing catalase, which is an antioxidant enzyme scavenging H_2O_2, resulted in a significant increase in catalase activity in the liver. Pre-injection of catalase-expressing Ad vectors dramatically prevented I/R-induced elevation in serum alanine aminotransferase (ALT) and aspartate aminotransferase (AST) levels, and hepatic necrosis. The livers were also protected in another liver injury model, CCl_4-induced liver injury, by catalase-expressing Ad vectors. Furthermore, the survival rates of mice subjected to both partial hepatectomy and I/R treatment were improved by pre-injection of catalase-expressing Ad vectors. On the other hand, control Ad vectors expressing β-galactosidase did not show any significant preventive effects in the liver on the models of I/R-induced or CCl_4-induced hepatic injury described above. These results indicate that hepatic delivery of the catalase gene by Ad vectors is a promising approach for the prevention of oxidative stress-induced liver injury.

1. Introduction

Hepatic ischemia/reperfusion (I/R) injury occurs in a variety of clinical settings, such as in liver transplantation, hepatic failure after shock, and liver surgery, and results in severe damages that substantially contribute to the morbidity and mortality of such cases [1–3]. Hepatic I/R injury is caused by reactive oxygen species (ROS), including superoxide anion, hydrogen oxide, and hydroxyl radical, which are generated by reperfusion of the ischemic tissue. ROS induce lipid peroxidation and damages to proteins and nucleic acids, leading to parenchymal cell dysfunction and necrosis, increased vascular permeability, and inflammatory cell infiltration [4]. Therefore, ROS should be detoxified to prevent hepatic I/R injury.

In previous animal studies, antioxidative enzyme catalase and superoxide dismutase (SOD) were systemically administered to neutralize ROS and prevent I/R-induced hepatic injury. Although catalase and SOD are endogenously expressed in the cells, the expression levels of these enzymes are insufficient to prevent I/R injury. Administration of antioxidant enzymes exhibited therapeutic effects on ROS-induced diseases, including I/R-induced hepatic injury, in several studies [5–8]; however, these enzymes are known to be rapidly eliminated from the circulation following systemic administration, which limits their therapeutic potential, [9,10] although chemical modification of antioxidant enzymes has been carried out to enhance their plasma half-lives and tissue accessibility [5,6,9]. In addition, systemically administered antioxidant enzymes might be degraded in the endosomes/lysosomes because they are internalized into the cells via the endocytosis pathway.

The delivery of therapeutic genes encoding antioxidant enzymes into the liver is considered to be a promising strategy to overcome these problems. Previous studies have demonstrated that ROS-mediated injury was efficiently prevented by over-expression of antioxidant

* Corresponding authors. Sakurai is to be contacted at Laboratory of Gene Transfer and Regulation, National Institute of Biomedical Innovation, 5-6-7 Saito Asagi, Ibaraki, Osaka, 567-0085, Japan. Tel.: +81 72 641 9815; fax: +81 72 641 9816. Mizuguchi, Department of Biochemistry and Molecular Biology, Graduate School of Pharmaceutical Sciences, Osaka University, 1-6 Yamadaoka, Suita, Osaka, 565-0871, Japan. Tel./fax: +81 6 6879 8185.
E-mail addresses: sakurai@nibio.go.jp (F. Sakurai), mizuguch@phs.osaka-u.ac.jp (H. Mizuguchi).

0168-3659/$ – see front matter.
doi:10.1016/j.jconrel.2009.11.024

enzymes in various tissues, including the artery, pancreatic islets, and brain [11–13]. A variety of types of gene delivery vehicles have been employed for delivery of antioxidative genes so far, and replication-incompetent adenovirus (Ad) vectors have several advantages over other vehicles to deliver antioxidant genes to the liver. First, Ad vectors have high tropism to livers. A more than 10^3-fold higher transgene expression is found in the liver, compared with other organs, following systemic administration [14–16]. Second, non-dividing cells are efficiently transduced with Ad vectors. Hepatocytes do not actively divide under normal conditions. Non-viral gene delivery vehicles have been used for prevention of hepatic I/R injury in previous studies [17,18]; however, non-viral gene delivery vehicles mediate inefficient transfection in non-dividing cells. Third, the Ad vector genome is not integrated into the host genome, indicating that transduction with Ad vectors is unlikely to induce insertional mutagenesis in hepatocytes. Fourth, Ad vector-mediated gene expression in liver persists for 1–2 weeks, [19,20] in contrast, rapid reduction in plasmid DNA-mediated transgene expression in organs is found after injection of non-viral gene delivery vehicles [21,22]. In spite of these advantages of Ad vectors, the ability of Ad vectors expressing antioxidant enzymes to prevent hepatic I/R injury has not been fully examined probably because Ad vectors are generally considered more toxic than non-viral gene delivery vehicles; however, our group demonstrated that intravenous administration of Ad vectors induces less amounts of inflammatory cytokines than cationic lipid/plasmid DNA complexes [23]. In addition, fiber-modified Ad vectors carrying a stretch of lysine residues in the C-terminus of a fiber knob have been demonstrated to poorly activate innate immune responses after systemic injection, compared with conventional Ad vectors [24]. These results suggest that Ad vectors, including fiber-modified Ad vectors, would be suitable for prevention of I/R injury by delivering antioxidant genes to livers.

Among antioxidant enzymes, SOD is often used for detoxifying ROS in previous studies [8,17,25,26]. SOD catabolizes superoxide anion to H_2O_2; however, H_2O_2 is converted to hydroxyl radicals, which are extremely reactive and more toxic than other ROS. H_2O_2 should be removed to effectively reduce I/R injury. Another antioxidant enzyme, catalase, prevents the generation of hydroxyl radicals by catabolizing H_2O_2 to H_2O and O_2, suggesting that catalase is promising for prevention of I/R injury. However, there are few studies reporting therapeutic effects of catalase gene delivery on I/R injury [17,27].

In the present study, catalase-expressing Ad vectors were intravenously pre-administered to prevent I/R-induced hepatic injury. Pre-injection of catalase-expressing Ad vectors successfully prevented not only I/R-induced hepatic injury but also CCl_4-induced liver damages. Furthermore, mice receiving pre-injection of catalase-expressing Ad vectors showed improved survival rates after partial hepatectomy followed by hepatic I/R.

2. Materials and methods

2.1. Cells

A549 (a human lung adenocarcinoma epithelial cell line), HepG2 (a human hepatocellular liver carcinoma cell line), and 293 (a human embryonic kidney cell line) cells were cultured in Dulbecco's modified Eagle's medium (DMEM) supplemented with 10% fetal bovine serum under 5% CO_2 at 37 °C.

2.2. Ad vectors

Ad vectors were constructed by means of an improved *in vitro* ligation method [28–30]. Briefly, the LacZ gene, which is derived from pCMVβ (Marker Gene, Inc., Eugene, OR) and the catalase gene, which is derived from pZEOSV2-CAT (a kind gift from Dr. J. Andres Melendez, Albany Medical College, Albany, NY) [31,32] were inserted into pHMCA5, [33] creating pHMCA5-LacZ and pHMCA5-CAT, respectively. pHMCA5-LacZ and pHMCA5-CAT were then digested with I-CeuI and PI-SceI, and ligated with I-CeuI/PI-SecI-digested pAdHM4 [28], resulting in pAdHM4-LacZ and pAdHM4-CAT, respectively. To generate the viruses, PacI-digested Ad vector plasmids were transfected into 293 cells plated in a 60-mm dish with SuperFect (Qiagen, Inc., Valencia, CA) according to the manufacturer's instructions. The viruses were prepared by the standard method, then purified with $CsCl_2$ gradient centrifugation, dialyzed with a solution containing 10 mM Tris (pH7.5), 1 mM $MgCl_2$, and 10% glycerol, and stored in aliquots at −80 °C. The determinations of infectious titers and virus particle (VP) titers were accomplished using 293 cells and an Adeno-X rapid titer kit (Clontech, Mountain View, CA) and the method of Maizel et al. [34], respectively. Catalase-, or β-galactosidase-expressing fiber-modified Ad vectors carrying a stretch of lysine residues (K7 (KKKKKKK) peptide) in the C-terminus of a fiber knob, AdK7-CAT and AdK7-LacZ, respectively, were similarly prepared using pAdHM41K7 [35]. The ratios of the biological-to-particle titer were 1:20, 1:31, 1:45, and 1:39 for Ad-LacZ, AdK7-LacZ, Ad-CAT, and AdK7-CAT, respectively.

2.3. Western blot analysis for catalase expression

A549 cells were transduced with Ad vectors at 3000 VP/cell for 2 h. Forty-eight hours later, cells were harvested and lysed with lysis buffer (20 mM Tris–HCl (pH 8.0), 137 mM NaCl, 1% Triton X-100, 10% glycerol) containing protease inhibitor cocktail (Sigma Chemical., St. Louis, MO). Equal quantities of protein (5 μg), as determined by a protein assay (Bio-Rad, Hercules, CA), were subjected to sodium dodecyl sulfate/12.5% polyacrylamide gel electrophoresis (SDS-PAGE) and transferred onto a polyvinylidene fluoride membrane (Millipore, Bedford, MA). After blocking nonspecific binding, the membrane was incubated with anti-catalase antibody (diluted 1/8000; Calbiochem, San Diego, CA) at room temperature for 3 h, followed by reaction with horse radish peroxidase (HRP)-conjugated anti-rabbit IgG (diluted 1/3000; Cell Signaling Technology, Beverly, MA) at room temperature for 1 h. The band was visualized by ECL Plus Western blotting detection reagents (Amersham Bioscience, Piscataway, NJ), and the signals were read using an LAS-3000 imaging system (Fujifilm, Tokyo, Japan). For detection of the internal control, a polyclonal anti-glyceraldehyde-3-phosphate dehydrogenase antibody (diluted 1/5000; Trevigen, Gaithersburg, MD) and an HRP-conjugated anti-rabbit IgG were used.

2.4. In vitro protective effect of catalase-expressing Ad vectors on ROS-induced cell damage

HepG2 cells (5000 cells/well) were seeded onto a 96-well plate. On the following day, the cells were transduced with Ad-LacZ, AdK7-LacZ, Ad-CAT, or AdK7-CAT at 300 or 3000 VP/cell for 2 h. After a 48-h incubation, the medium was exchanged for normal medium containing 30 mM menadione (Sigma Chemical), which is a ROS inducer. On the following day, the cell viability was determined by Alamar blue staining (BioSource, San Diego, CA).

2.5. Catalase activities in the liver after intravenous administration of Ad vectors

Ad vectors (Ad-LacZ, AdK7-LacZ, Ad-CAT, and AdK7-CAT) were intravenously administered into C57BL/6 mice (7–8-week-old females; Nippon SLC, Shizuoka, Japan) at a dose of 1×10^{10} VP/mice. Forty-eight hours later, the livers were isolated and homogenized with 50 mM potassium phosphate buffer containing 1 mM EDTA. The supernatants were recovered after centrifugation of the homogenates, and catalase activity in the supernatants was measured using a CalBiochem Catalase Assay Kit (Calbiochem).

2.6. Hepatic ischemia/reperfusion experiment

Mice were intravenously administered PBS (control) or Ad vectors via the tail vein at a dose of 10^{10} VP/mice. A partial hepatic ischemia/reperfusion experiment was performed as previously described [36,37]. Briefly, 2 days post-administration of Ad vectors, mice were anesthetized with a peritoneal injection of pentobarbital sodium (50 mg/kg). An incision was made in the abdomen, and all structures in the portal triad (hepatic artery, portal vein, bile duct) were occluded with a vascular clamp for 1 h to induce hepatic ischemia. Then, blood was allowed to flow through the liver again by removal of the clamp (reperfusion). After an appropriate period of reperfusion (0, 1, 6, 24 h), blood was collected via retro-orbital bleeding, and serum was obtained by centrifugation. The aspartate aminotransferase (ALT) and alanine aminotransferase (AST) activities in serum, as indicators of liver injury during reperfusion, were assayed using a transaminase-CII test (Wako, Osaka, Japan). In separate experiments, histology in the liver sections was evaluated 24 h after reperfusion. The livers were recovered and fixed by immersion in 10% buffered formalin, embedded in paraffin and processed for histology. Tissue damage was assessed in hematoxylin and eosin-stained sections. A sham surgery was performed under anesthesia but without occluding the vessels.

2.7. CCl_4-induced liver injury experiment

Ad vectors were intravenously administered into mice as described above. Forty-eight hours after Ad vector injection, CCl_4 dissolved in olive oil was intraperitoneally administrated to the mice at a dose of 1 ml/kg body weight to induce acute liver failure. Twenty-four hours after CCl_4 administration, blood was collected via retro-orbital bleeding, and the levels of ALT and AST in the serum were determined as described above.

2.8. Partial hepatectomy

Ad vectors were intravenously administered into mice as described above. Forty-eight hours after Ad vector injection, mice were anesthetized and subjected to two-thirds hepatectomy as described previously [38,39]. Subsequently, liver I/R was conducted by occlusion of the blood vessel to block the blood flow into the remnant liver for 8 min followed by reperfusion as described above. After the surgery, the mice were maintained under conventional conditions to monitor survival rates.

2.9. Statistical analysis

Results were expressed as the means ± S.D. Statistically significant differences between groups were determined by the two-way analysis of variance, followed by Student's *t*-test. The levels of statistical significance were set at $p<0.05$ and $p<0.01$.

3. Results

3.1. Ad vector-mediated catalase expression in vitro

First, to examine *in vitro* catalase expression levels following Ad vector infection, Western blotting analysis was performed. We observed an apparent increase in the catalase expression after transduction with Ad-CAT or AdK7-CAT in A549 cells (Fig. 1). In addition, AdK7-CAT mediated higher catalase expression than Ad-CAT, probably due to the higher transduction activity of AdK7 vectors than conventional Ad vectors [35]. The control Ad vectors, Ad-LacZ and AdK7-LacZ, did not increase catalase expression, indicating that transduction with Ad vectors alone does not induce any change in the antioxidant systems.

Next, to examine whether Ad vector-mediated over-expression of catalase prevents ROS-induced cellular toxicity, the cells were incubated with 30 mM menadione following transduction with Ad vectors, and the cell viabilities were determined. It is well known that menadione produces superoxide radicals in cells, leading to oxidative stress-induced cell death [40,41]. As shown in Fig. 2, the cell viability was significantly reduced to less than 50% in the presence of 30 mM menadione. In contrast, transduction with catalase-expressing Ad vectors dramatically improved the cell viabilities. Transduction with Ad-CAT and AdK7-CAT at 300 VP/cell resulted in cell viabilities of 70.8% and 79.1% of the cell, respectively. These results indicate that Ad vector-mediated over-expression of catalase is beneficial in preventing oxidative stress-induced cell death by efficiently deleting ROS.

3.2. Catalase activity in the liver following catalase-expressing Ad vector injection

Next, to measure catalase activities in the liver following intravenous administration of Ad vectors, the livers were recovered 48 h after Ad vector injection, and catalase activities in the liver were determined. The catalase activities were 2.4-fold and 4.3-fold increased following administration of Ad-CAT and AdK7-CAT, respectively (Fig. 3). By contrast, we found no elevation in the catalase activity by LacZ-expressing Ad vectors. These results indicate that catalase activity in the liver is significantly elevated by intravenous administration of catalase-expressing Ad vectors.

3.3. Prevention of hepatic I/R injury by pre-administration of catalase-expressing Ad vectors

To evaluate the ability of catalase-expressing Ad vectors to prevent hepatic I/R injury, serum ALT and AST levels were measured after 1 h of hepatic ischemia followed by reperfusion. Both serum ALT and AST levels were highly elevated at 1 h and 6 h after the reperfusion of hepatic flows in the mice pre-injected with PBS, indicating that hepatic injury was induced by I/R (Fig. 4). At 1 h after reperfusion, the ALT and AST levels increased from 59.3 to 184.0 and from 421.2 to 1174.7 IU/L, respectively. However, pretreatment with Ad-CAT or AdK7-CAT significantly reduced the serum ALT and AST levels at 6 h after reperfusion. The ALT and AST levels in mice pre-injected with AdK7-CAT were 3.9- and 4.4-fold lower than those in mice pre-injected with PBS. Reductions in the ALT and AST levels were also observed at 1 h after reperfusion, although these changes were not statistically significant. The control Ad vectors, Ad-LacZ and AdK7-LacZ, exhibited no suppressive effects on the I/R-induced elevation of serum ALT and AST levels.

Furthermore, to histologically evaluate the preventive effects of catalase-expressing Ad vectors, liver sections were prepared 24 h after reperfusion. An extensive necrotic area was observed in the mice pretreated with PBS or AdK7-LacZ (Fig. 5B, C). In contrast, transduction with Ad-CAT or AdK7-CAT resulted in a dramatic decrease in the necrotic area induced by hepatic I/R (Fig. 5D, E). In particular,

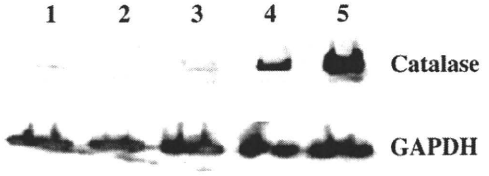

Fig. 1. Catalase expression following Ad vector transduction. A549 cells were transduced with Ad-LacZ, Ad-CAT, or AdK7-CAT at 3000 VP/cell for 2 h. Protein samples were collected after a 48-h incubation and analyzed by Western blotting. Lane 1, mock; lane 2, Ad-LacZ; lane 3, AdK7-LacZ; lane 4, Ad-CAT; lane 5, AdK7-CAT. The results are representative of two

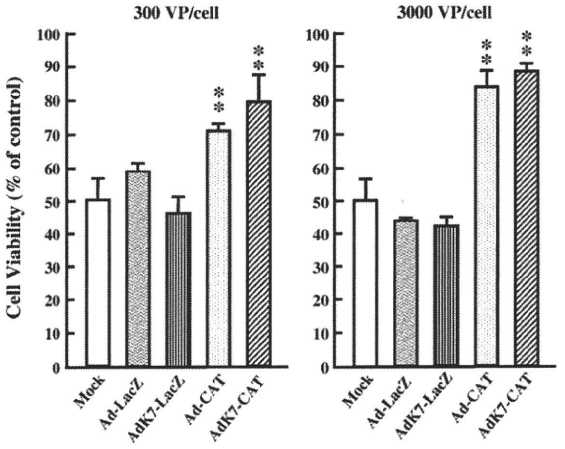

Fig. 2. Protective effects of catalase-expressing Ad vectors against menadione-induced cell death. HepG2 cells were transduced with Ad vectors at 300 or 3000 VP/cell for 2 h. After a 48-h incubation, menadione was added to the medium at a final concentration of 30 mM, and the cells were cultured for an additional 24 h. The cellular viabilities were then determined by Alamar blue staining. The cellular viabilities were normalized to the viability of Ad vector-infected HepG2 cells in the absence of menadione. The data are expressed as the means ± S.D. ($n=4$). **Significantly different from the mock-infected group at $p<0.01$.

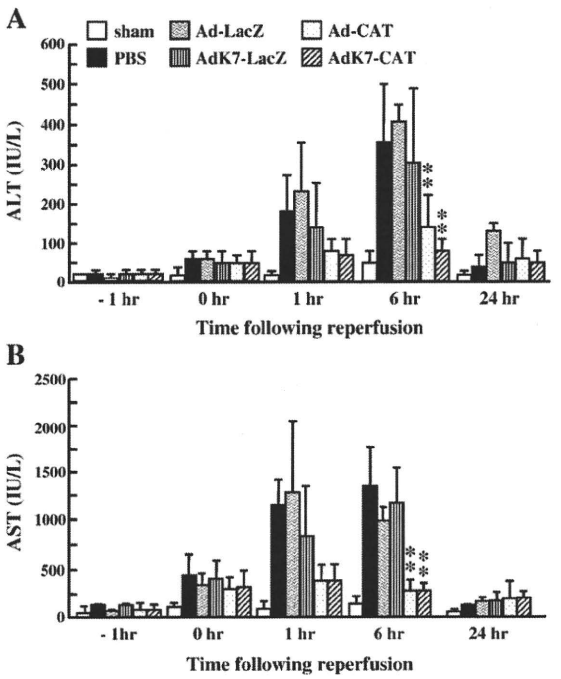

Fig. 4. Effects of pre-administration of catalase-expressing Ad vectors on serum ALT (A) and AST (B) levels in mice following hepatic ischemia/reperfusion injury. Ad vectors were intravenously administered to mice at a dose of 1×10^{10} VP/mice. Forty-eight hours after Ad vector injection, mice were subjected to a 1 h period of ischemia followed by hepatic reperfusion. Serum samples were taken at 1 h before ischemia, and 0, 1, 6, and 24 h after reperfusion. The data are expressed as the mean ± S.E. ($n=3$–8). **Significantly different from the PBS-injected group at $p<0.01$.

pre-injection of AdK7-CAT almost completely prevented necrosis in the liver, although there were several small necrotic areas in the liver pretreated with Ad-CAT, probably due to the higher transduction efficiency and less liver toxicity profile of AdK7 vectors in the liver compared with conventional Ad vectors [24]. A TUNEL assay indicated that Ad-CAT and AdK7-CAT prevented the DNA fragmentation caused by hepatic I/R in hepatocytes (data not shown). These results indicate that the I/R-induced histological damages were also significantly attenuated by pretreatment with catalase-expressing Ad vectors.

3.4. Preventive effect of catalase-expressing Ad vectors on CCl_4-induced liver injury

To explore whether Ad vector-mediated catalase expression prevents other types of oxidative stress-induced liver injury, CCl_4 was intraperitoneally injected into mice pretreated with catalase-expressing Ad vectors. CCl_4 is well known to produce CCl_3 radical, leading to acute liver injury. Serum ALT and AST levels were highly elevated following CCl_4 treatment in mice pretreated with PBS or LacZ-expressing Ad vectors (Fig. 6). However, serum ALT and AST levels were markedly reduced by pretreatment with Ad-CAT and AdK7-CAT. AdK7-CAT mediated a 4.9-fold and 3.9-fold reduction in serum ALT and AST levels, respectively, compared with PBS. Ad-CAT and AdK7-CAT also mediated a dramatic improvement of CCl_4-induced gross abnormality in the liver (data not shown). These results indicate that catalase-expressing Ad vectors possess preventive effects on oxidative stress-induced injury that are distinct from their effects on I/R injury.

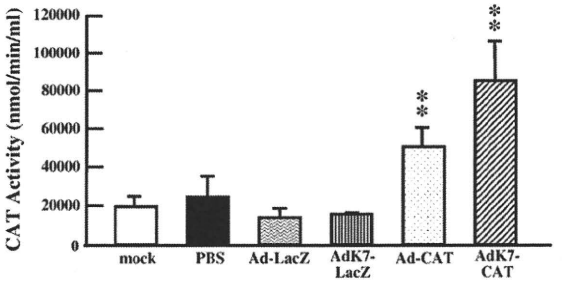

Fig. 3. Catalase activity in the liver following intravenous administration of catalase-expressing Ad vectors. Ad vectors were administered to mice at the dose of 1×10^{10} VP/mouse. The livers were recovered 48 h after injection, and catalase activities in mouse liver homogenates were determined. The data are expressed as the means ± S.D. ($n=5$). **Significantly different from the mock-infected group at $p<0.01$.

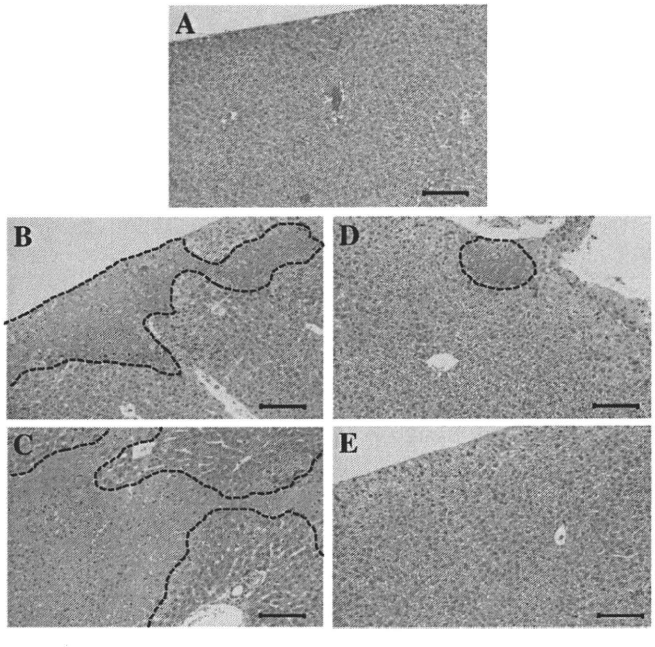

Fig. 5. Representative images of liver sections of mice 24 h following hepatic ischemia/reperfusion. A) Sham, B) PBS, C) AdK7-LacZ, D) Ad-CAT, and E) AdK7-CAT. Mice were subjected to hepatic I/R 48 h after Ad vector injection, as described in Fig. 4. Livers were recovered 24 h after I/R treatment, and liver sections stained with hematoxylin and eosin were observed under a microscope. A dashed line indicates the necrotic area. The scale bar represents 100 μm.

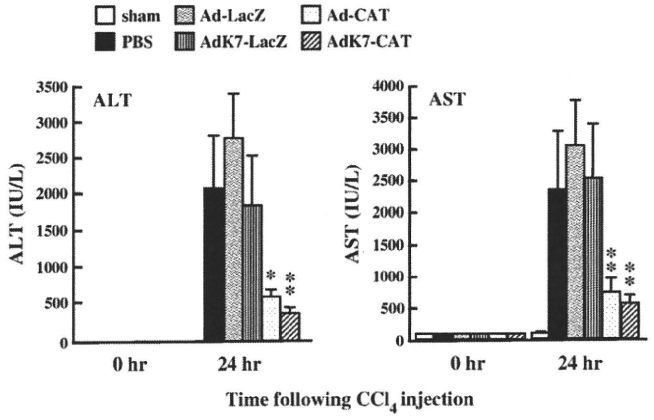

Fig. 6. Preventive effect of catalase-expressing Ad vectors on CCl_4-induced acute liver failure. CCl_4 (1 ml/kg) was intraperitoneally injected to mice 48 h following Ad vector injection. Serum samples were collected 24 h after CCl_4 administration. The data are expressed as the means ± S.D. ($n=4$). *Significantly different from the PBS-injected group at $p<0.05$; ** at $p<0.01$.

3.5. Improvement of survival rates of mice subjected to partial hepatectomy and hepatic ischemia/reperfusion by catalase-expressing Ad vectors

To examine whether over-expression of catalase improves the remnant liver function in mice subjected to both partial hepatectomy and I/R treatment, partial hepatectomy and subsequent I/R treatment were conducted 48 h after pre-administration of Ad vectors. Partial hepatectomy is often performed under hepatic ischemia, and the remaining liver suffers from I/R injury after partial hepatectomy in clinical settings. Mice pre-administered with AdK7-CAT showed a dramatic improvement in survival rate (Fig. 7). Seventy percent of mice survived for 7 days after these treatments. The body weights of the mice pre-injected with AdK7-CAT were not significantly reduced 7 days after surgery, compared with those before surgery (data not shown), suggesting that the general health of the mice was not substantially compromised after the surgery. On the other hand, the survival of the mice was not prolonged by pre-administration of Ad-LacZ or PBS. These results indicate that catalase-expressing Ad vectors are able to protect the liver from more serious stress induced by partial hepatectomy and I/R, and to improve the remnant liver function.

4. Discussion

Hepatotoxins, drugs, and I/R can injure the liver via oxidative stress. With the aim of efficiently preventing oxidative stress-induced hepatic injury, we pre-administered Ad vectors expressing an antioxidative enzyme, catalase, to mice. The results of our study demonstrated that Ad vector-mediated over-expression of catalase in the liver effectively prevents hepatic injury caused by not only I/R but also CCl_4. Furthermore, the survival rates of mice subjected to both partial hepatectomy and I/R treatment were prolonged by over-expression of catalase.

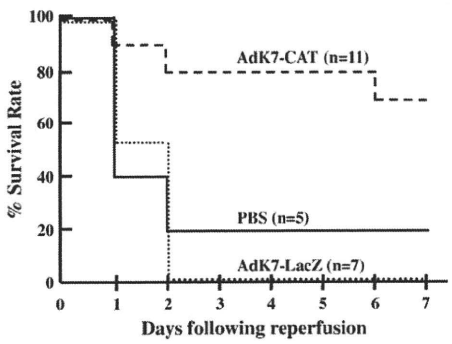

Fig. 7. Survival rates of mice subjected to partial hepatectomy and hepatic I/R following Ad vector administration. Solid line: PBS ($n=5$); dotted line: AdK7-LacZ ($n=7$); dashed line: AdK7-CAT ($n=11$). Ad vectors were intravenously administered to mice as described in Fig. 4. Forty-eight hours after Ad vector administration, mice were subjected to two-thirds partial hepatectomy, followed by an 8 min-period of ischemia

Superoxide anion is the primary oxidant species generated during hepatic I/R by a xanthine oxidase system and/or decoupling of the electron transport system in mitochondria. Superoxide anion is readily converted to H_2O_2 by SOD or a spontaneous reaction. H_2O_2 itself is a weak oxidizing agent; however, hydroxyl radical is produced by H_2O_2 in the presence of transition-metal ion. Hydroxyl radical has the most oxidative ability and the strongest toxicity among the various ROS. Reduction/elimination of hydroxyl radical is considered to be the most effective strategy for prevention of hepatic I/R injury. Therefore, catalase, which prevents generation of hydroxyl radical by converting H_2O_2 to H_2O and O_2, was selected as the antioxidant enzyme in the present study. Catalase derivatives also exhibited higher preventive effects on the elevation of serum ALT and AST levels induced by hepatic I/R, compared with SOD derivatives [5,6]. In addition, over-expression of catalase in the liver might increase endogenous expression of SOD, which is another advantage of catalase gene transfer. He et al. demonstrated that delivery of catalase gene alone to the liver induced SOD activity in the liver [17].

Partial hepatectomy is often performed under hepatic ischemia. Previous studies have shown that oxidative stress induced by hepatic I/R affects hepatocyte cell death and inhibits liver regeneration [42,43]. Beyer et al. reported that ROS are directly responsible for the impairment of insulin/insulin-like growth factor 1 signaling, which is crucial for liver regeneration [44]. Furthermore, hepatocytes without catalase activity have been found in regenerating livers after partial hepatectomy [45], suggesting that hepatocytes in the regenerating livers might be susceptible for ROS-mediated injury. The present study demonstrated that over-expression of catalase in the liver dramatically improved the survival rates of mice subjected to partial hepatectomy and I/R, suggesting that the remnant livers would be protected from ROS-mediated injury by over-expression of catalase. Furthermore, over-expression of catalase might play an important role in maintenance of the regenerative capacity of hepatocytes. Recently, removal of ROS by antioxidant enzymes was demonstrated to be crucial for maintenance of the self-renewal capacity of progenitor/stem cells in an *in vitro* culture system [46,47]. In this study, the liver/body weight ratio of mice pre-injected with AdK7-CAT 1 week after partial hepatectomy and I/R was 4.7 ± 0.55%, which is not significantly different from that of naïve mice (data not shown).

Oxidative stress is also generated in the liver through metabolism of a variety of drugs, chemicals, and toxins, such as thioacetamide, lipopolysaccharide, and CCl_4. In particular, CCl_4 is often used as a representative hepatotoxin causing oxidative stress in animal experiments. CCl_4 is metabolized by cytochrome P450 in the endoplasmic reticulum of hepatocytes, leading to generation of CCl_3 radical, which induces hepatic damages, although the mechanism of CCl_4-mediated liver damage has not yet been fully revealed. The present study showed that Ad vector-mediated over-expression of catalase in the liver also attenuated CCl_4-induced liver injury (Fig. 6). Over-expression of SOD has also been shown to inhibit CCl_4-induced hepatic damages [48]. Hepatic delivery of genes encoding ROS-deleting enzymes is effective in case of hepatic injury induced by oxidative stress-generating hepatotoxins and chemical compounds.

Ad vectors offer various advantages for gene delivery to the liver; however, systemic administration of Ad vectors often induces inflammatory cytokine production and hepatic damage [24,49–51]. However, we found no apparent Ad vector-induced damages in the liver in this study (data not shown). Moreover, mice pre-administered Ad-LacZ or AdK7-LacZ did not exhibit higher levels of serum ALT and AST after I/R than those pre-administered PBS (Fig. 4). This was likely

due to the relatively low dose of Ad vectors (1×10^{10} VP/mouse) used in this study. Higher doses of Ad vectors have often been administered in the studies reporting Ad vector-mediated *in vivo* toxicities [49,51]. We confirmed that more than 90% of hepatocytes were efficiently transduced even at a dose of 1×10^{10} VP/mouse in this study (data not shown). In general, Ad vectors have been considered more toxic than non-viral vectors containing plasmid DNA; however, our group recently revealed that Ad vectors induced smaller amounts of inflammatory cytokines, which are partly involved in Ad vector-induced hepatic toxicity, following intravenous administration into mice, compared with plasmid DNA/cationic liposome complexes, which were used as a representative of non-viral gene delivery vehicle [23]. In both that previous study and our present work, Ad vectors successfully deliver antioxidant genes to the liver with no apparent toxicity, although we should pay attention to the vector doses.

In addition to conventional Ad vectors, fiber-modified AdK7 vectors, which display a poly-lysine motif on the c-terminal of the fiber knob, [24,35,52] were used in this study. AdK7 vectors mediate not only significantly higher transgene expression in the liver but also lower *in vivo* damages than conventional Ad vectors [24]. However, the serum ALT and AST levels of the mice receiving Ad-CAT and AdK7-CAT were not significantly different from those of the controls in this study (Fig. 4), although histological analysis of the liver sections revealed that AdK7-CAT conferred superior protection against I/R injury (Fig. 5), probably because sufficient levels of catalase would be expressed by Ad-CAT at this dose to prevent hepatic I/R-induced increases in serum ALT and AST in this setting. AdK7-CAT might show higher protective effects than conventional Ad vectors under more severe conditions.

In conclusion, the present study demonstrated that Ad vector-mediated catalase expression in the liver significantly improved I/R-induced hepatic injury. These findings suggests that Ad vectors expressing antioxidant enzymes would contribute to the development of strategies aimed at inhibiting hepatic I/R injury. Antioxidant enzyme-expressing Ad vectors are also applicable for the prevention of I/R-induced injury in other organs and oxidative stress-induced damages caused by ROS-generating chemicals. Moreover, their combined use with other antioxidant genes or anti-apoptosis genes could further attenuate oxidative stress-induced injury.

Acknowledgement

We thank Dr. Yuriko Higuchi (Graduate School of Pharmaceutical Sciences, Kyoto University, Kyoto, Japan) for her help in the liver ischemia/reperfusion experiments. We also thank Dr. Kazuo Ohashi (Institute of Advanced Biomedical Engineering and Sciences, Tokyo Women's Medical University, Tokyo, Japan) for his help in the partial hepatectomy experiment. This work was supported by grants from the Ministry of Health, Labour, and Welfare of Japan.

References

[1] R.G. Thurman, et al., Hepatic reperfusion injury following orthotopic liver transplantation in the rat, Transplantation 46 (1988) 502–506.
[2] J.M. McCord, Oxygen-derived free radicals in postischemic tissue injury, N. Engl. J. Med. 312 (1985) 159–163.
[3] M.J. Arthur, et al., Oxygen-derived free radicals promote hepatic injury in the rat, Gastroenterology 89 (1985) 1114–1122.
[4] D.N. Granger, R.J. Korthuis, Physiologic mechanisms of postischemic tissue injury, Annu. Rev. Physiol. 57 (1995) 311–332.
[5] Y. Yabe, et al., Prevention of neutrophil-mediated hepatic ischemia/reperfusion injury by superoxide dismutase and catalase derivatives, J. Pharmacol. Exp. Ther. 298 (2001) 894–899.
[6] Y. Yabe, et al., Targeted delivery and improved therapeutic potential of catalase by chemical modification: combination with superoxide dismutase derivatives, J. Pharmacol. Exp. Ther. 289 (1999) 1176–1184.
[7] S.L. Atalla, L.H. Toledo-Pereyra, G.H. MacKenzie, J.P. Cederna, Influence of oxygen-derived free radical scavengers on ischemic livers, Transplantation 40 (1985) 584–590.
[8] T. Fujita, et al., Therapeutic effects of superoxide dismutase derivatives modified with mono- or polysaccharides on hepatic injury induced by ischemia/reperfusion, Biochem. Biophys. Res. Commun. 189 (1992) 191–196.
[9] P.S. Pyatak, A. Abuchowski, F.F. Davis, Preparation of a polyethylene glycol: superoxide dismutase adduct, and an examination of its blood circulation life and anti-inflammatory activity, Res. Commun. Chem. Pathol. Pharmacol. 29 (1980) 113–127.
[10] J.F. Turrens, J.D. Crapo, B.A. Freeman, Protection against oxygen toxicity by intravenous injection of liposome-entrapped catalase and superoxide dismutase, J. Clin. Invest. 73 (1984) 87–95.
[11] L. Agrawal, et al., Antioxidant enzyme gene delivery to protect from HIV-1 gp120-induced neuronal apoptosis, Gene Ther. 13 (2006) 1645–1656.
[12] P.Y. Benhamou, et al., Adenovirus-mediated catalase gene transfer reduces oxidant stress in human, porcine and rat pancreatic islets, Diabetologia 41 (1998) 1093–1100.
[13] E. Durand, et al., Adenovirus-mediated gene transfer of superoxide dismutase and catalase decreases restenosis after balloon angioplasty, J. Vasc. Res. 42 (2005) 255–265.
[14] F. Sakurai, H. Mizuguchi, T. Yamaguchi, T. Hayakawa, Characterization of in vitro and in vivo gene transfer properties of adenovirus serotype 35 vector, Mol. Ther. 8 (2003) 813–821.
[15] H. Mizuguchi, et al., CAR- or alphav integrin-binding ablated adenovirus vectors, but not fiber-modified vectors containing RGD peptide, do not change the systemic gene transfer properties in mice, Gene Ther. 9 (2002) 769–776.
[16] R. Alemany, D.T. Curiel, CAR-binding ablation does not change biodistribution and toxicity of adenoviral vectors, Gene Ther. 8 (2001) 1347–1353.
[17] S.Q. He, et al., Delivery of antioxidative enzyme genes protects against ischemia/reperfusion-induced liver injury in mice, Liver Transpl. 12 (2006) 1869–1879.
[18] H. Yin, et al., Pretreatment with soluble ST2 reduces warm hepatic ischemia/reperfusion injury, Biochem. Biophys. Res. Commun. 351 (2006) 940–946.
[19] R.S. Sung, L. Qin, J.S. Bromberg, TNFalpha and IFNgamma induced by innate anti-adenoviral immune responses inhibit adenovirus-mediated transgene expression, Mol. Ther. 3 (2001) 757–767.
[20] N. Morral, et al., Immune responses to reporter proteins and high viral dose limit duration of expression with adenoviral vectors: comparison of E2a wild type and E2a deleted vectors, Hum. Gene Ther. 8 (1997) 1275–1286.
[21] S. Li, L. Huang, In vivo gene transfer via intravenous administration of cationic lipid–protamine–DNA (LPD) complexes, Gene Ther. 4 (1997) 891–900.
[22] S. Li, et al., Effect of immune response on gene transfer to the lung via systemic administration of cationic lipidic vectors, Am. J. Physiol. 276 (1999) L796–L804.
[23] H. Sakurai, et al., Comparison of gene expression efficiency and innate immune response induced by Ad vector and lipoplex, J. Control. Release 117 (2007) 430–437.
[24] N. Koizumi, et al., Fiber-modified adenovirus vectors decrease liver toxicity through reduced IL-6 production, J. Immunol. 178 (2007) 1767–1773.
[25] M.D. Wheeler, et al., Comparison of the effect of adenoviral delivery of three superoxide dismutase genes against hepatic ischemia–reperfusion injury, Hum. Gene Ther. 12 (2001) 2167–2177.
[26] S. Kondo, et al., Mannosylated superoxide dismutase inhibits hepatic reperfusion injury in rats, J. Surg. Res. 60 (1996) 36–40.
[27] B. Chen, et al., Delivery of antioxidant enzyme genes protects against ischemia/reperfusion-induced injury to retinal microvasculature, Invest. Ophthalmol. Vis. Sci. 50 (2009) 5587–5595.
[28] H. Mizuguchi, M.A. Kay, Efficient construction of a recombinant adenovirus vector by an improved in vitro ligation method, Hum. Gene Ther. 9 (1998) 2577–2583.
[29] H. Mizuguchi, M.A. Kay, A simple method for constructing E1- and E1/E4-deleted recombinant adenoviral vectors, Hum. Gene Ther. 10 (1999) 2013–2017.
[30] H. Mizuguchi, et al., A simplified system for constructing recombinant adenoviral vectors containing heterologous peptides in the HI loop of their fiber knob, Gene Ther. 8 (2001) 730–735.
[31] M. Mari, J. Bai, A.I. Cederbaum, Adenovirus-mediated overexpression of catalase in the cytosolic or mitochondrial compartment protects against toxicity caused by glutathione depletion in HepG2 cells expressing CYP2E1, J. Pharmacol. Exp. Ther. 301 (2002) 111–118.
[32] J. Bai, A.I. Cederbaum, Adenovirus-mediated overexpression of catalase in the cytosolic or mitochondrial compartment protects against cytochrome P450 2E1-dependent toxicity in HepG2 cells, J. Biol. Chem. 276 (2001) 4315–4321.
[33] F. Sakurai, et al., Optimization of adenovirus serotype 35 vectors for efficient transduction in human hematopoietic progenitors: comparison of promoter activities, Gene Ther. 12 (2005) 1424–1433.
[34] J.V. Maizel Jr., D.O. White, M.D. Scharff, The polypeptides of adenovirus. I. Evidence for multiple protein components in the virion and a comparison of types 2, 7A, and 12, Virology 36 (1968) 115–125.
[35] N. Koizumi, et al., Generation of fiber-modified adenovirus vectors containing heterologous peptides in both the HI loop and C terminus of the fiber knob, J. Gene Med. 5 (2003) 267–276.
[36] A. Tsung, et al., The nuclear factor HMGB1 mediates hepatic injury after murine liver ischemia–reperfusion, J. Exp. Med. 201 (2005) 1135–1143.
[37] M.R. Duranski, et al., Cytoprotective effects of nitrite during in vivo ischemia–reperfusion of the heart and liver, J. Clin. Invest. 115 (2005) 1232–1240.
[38] K. Ohashi, F. Park, M.A. Kay, Role of hepatocyte direct hyperplasia in lentivirus-mediated liver transduction in vivo, Hum. Gene Ther. 13 (2002) 653–663.
[39] K. Ohashi, et al., Liver tissue engineering at extrahepatic sites in mice as a potential new therapy for genetic liver diseases, Hepatology 41 (2005) 132–140.
[40] T.J. Monks, et al., Quinone chemistry and toxicity, Toxicol. Appl. Pharmacol. 112 (1992) 2–16.
[41] H. Thor, et al., The metabolism of menadione (2-methyl-1, 4-naphthoquinone) by isolated hepatocytes. A study of the implications of oxidative stress in intact cells, J. Biol. Chem. 257 (1982) 12419–12425.
[42] N. Fausto, Liver regeneration, J. Hepatol. 32 (2000) 19–31.

[43] H. Kamata, et al., Reactive oxygen species promote TNFalpha-induced death and sustained JNK activation by inhibiting MAP kinase phosphatases, Cell 120 (2005) 649–661.
[44] T.A. Beyer, et al., Impaired liver regeneration in Nrf2 knockout mice: role of ROS-mediated insulin/IGF-1 resistance, Embo J. 27 (2008) 212–223.
[45] I. Oikawa, P.M. Novikoff, Catalase-negative peroxisomes: transient appearance in rat hepatocytes during liver regeneration after partial hepatectomy, Am. J. Pathol. 146 (1995) 673–687.
[46] R.C. Meagher, A.J. Salvado, D.G. Wright, An analysis of the multilineage production of human hematopoietic progenitors in long-term bone marrow culture: evidence that reactive oxygen intermediates derived from mature phagocytic cells have a role in limiting progenitor cell self-renewal, Blood 72 (1988) 273–281.
[47] R. Gupta, S. Karpatkin, R.S. Basch, Hematopoiesis and stem cell renewal in long-term bone marrow cultures containing catalase, Blood 107 (2006) 1837–1846.
[48] S.K. Venugopal, et al., Lentivirus-mediated superoxide dismutase1 gene delivery protects against oxidative stress-induced liver injury in mice, Liver Int. 27 (2007) 1311–1322.
[49] M. Christ, et al., Modulation of the inflammatory properties and hepatotoxicity of recombinant adenovirus vectors by the viral E4 gene products, Hum. Gene Ther. 11 (2000) 415–427.
[50] A. Lieber, et al., Inhibition of NF-kappaB activation in combination with bcl-2 expression allows for persistence of first-generation adenovirus vectors in the mouse liver, J. Virol. 72 (1998) 9267–9277.
[51] R.S. Everett, et al., Liver toxicities typically induced by first-generation adenoviral vectors can be reduced by use of E1, E2b-deleted adenoviral vectors, Hum. Gene Ther. 14 (2003) 1715–1726.
[52] T.J. Wickham, et al., increased in vitro and in vivo gene transfer by adenovirus vectors containing chimeric fiber proteins, j. virol. 71 (1997) 8221–8229.

PharmSight™
DOI: 10.4255/mcpharmacol.10.07

Molecular and Cellular Pharmacology
www.mcpharmacol.com

Potency of Claudin-targeting as Antitumor Therapy

Rie Saeki[1], Masuo Kondoh[1], Hiroshi Uchida[2] and Kiyohito Yagi[1]

[1]Laboratory of Bio-Functional Molecular Chemistry, Graduate School of Pharmaceutical Sciences, Osaka University, Osaka 565-0871, Japan; [2]Department of Biopharmaceuticals Research, Biopharma Center, Asubio Pharma Co., Ltd., Gunma 370-0503, Japan

PharmSight on Saeki R et al., A novel tumor-targeted therapy using a claudin-4-targeting molecule. Mol Pharmacol 2009;76:918-26.

Abstract

Approximately 90% of malignant tumors are derived from the epithelium. Epithelium has well-developed tight junctions (TJs), which become deregulated and disrupted during epithelial transformation. Claudin-4, a pivotal functional and structural component of TJs, is often overexpressed in human cancers. In the present study, we prepared a claudin-4 binder, the C-terminal fragment of *Clostridium perfringens* enterotoxin (C-CPE), fused to a cytotoxic molecule (C-CPE-PSIF) and found that C-CPE-PSIF is toxic to claudin-4-expressing cells. Interestingly, C-CPE-PSIF was less toxic in polarized than depolarized cells, and treatment of polarized cells with C-CPE-PSIF from the basal but not apical side was cytotoxic. C-CPE-PSIF also exhibits antitumor activity. C-CPE mutants with alanine substitutions were more cytotoxic than C-CPE. These findings indicate that the claudin-4 binder, C-CPE, is a potent lead molecule for the development of claudin-targeted tumor therapy.

Keywords: Claudin; *Clostridium perfringens* enterotoxin; *Pseudomonas* exotoxin; Anti-tumor activity

Introduction

Tight junctions (TJs) consist of three main classes of proteins: claudins, occludin, and junctional adhesion molecules. Claudins regulate the integrity and function of TJs (1). The human family of claudin proteins contains at least 23 members, and their expression profiles and functions are tissue and cell specific (2). Changes in claudin expression occur in malignant tumors, and the expression profiles differ among tissues (3, 4). For example, claudin-1 and -10 are overexpressed in colon and hepatocellular cancer cells, respectively (3), while claudin-4 is up-regulated in breast, ovarian, pancreatic, colorectal, hepatic and bladder cancers (Table 1). Thus, claudins are potential targets for tumor therapy. However, claudin has low antigenicity, and it is difficult to generate antibodies to the extracellular region of claudins.

Clostridium perfringens enterotoxin (CPE) is a single polypeptide of 35 kDa that causes food poisoning in humans. The functional domains of CPE are classified into the N-terminal cytotoxic and C-terminal receptor-binding regions (5, 6). Two years after the CPE receptor was identified in 1997, it was found to be identical to claudin-4 (7, 8). Interestingly, C-terminal CPE, which corresponds to amino acids 184 to 319 ($C\text{-}CPE_{184\text{-}319}$), binds to claudin-4 and inhibits TJ function. We previously found that $C\text{-}CPE_{184\text{-}319}$ is a useful ligand for claudin-4 (9). However, $C\text{-}CPE_{184\text{-}319}$ has poor solubility (0.3 mg/ml) and is difficult to use in pharmaceutical therapy. In 2008, Van Itallie et al. showed that a slightly smaller polypeptide, $C\text{-}CPE_{194\text{-}319}$, has high solubility (>10 mg/ml) and high affinity to claudin-4 (10).

Pseudomonas aeruginosa exotoxin A (PE) is widely used in cancer-targeting study (11). PE binds to the cell surface and is internalized via endocytosis; then, a PE fragment, protein synthesis inhibitory factor (PSIF), escapes from the endosome to the cytosol (12), where it inhibits protein synthesis by inhibiting elongation factor 2. PSIF lacks the receptor-binding domain of PE, and fusion of a tumor

Received 11/25/09; accepted 02/24/10

Correspondence: Dr. Masuo Kondoh, Laboratory of Bio-Functional Molecular Chemistry, Graduate School of Pharmaceutical Sciences, Osaka University, Suita, Osaka 565-0871, Japan. Tel. 81-6-6879-8196, Fax. 81-6-6879-8199. e-mail: masuo@phs.osaka-u.ac.jp; Dr. Kiyohito Yagi, Laboratory of Bio-Functional Molecular Chemistry, Graduate School of Pharmaceutical Sciences, Osaka University, Suita, Osaka 565-0871, Japan. Tel. 81-6-6879-8195, Fax. 81-6-6879-8195. e-mail: yagi@phs.osaka-u.ac.jp

Table 1 Changes in expression of claudin-4 in cancer cells

Cancer	Expression	References
Prostate	Up	(25)
Breast	Up	(26, 27)
Ovarian	Up	(28-31)
Pancreatic	Up	(32-34)
Colorectal	Up	(35)
Uterus	UP	(36, 37)
Gastric	Down	(38, 39)
Hepatocellular	Up	(40)

antigen ligand with PSIF is a promising strategy for cancer-targeting therapy.

In the present study, we genetically prepared a claudin-4-targeting molecule (C-CPE$_{194-319}$-PSIF) containing the claudin-4-binding region of CPE and PSIF (Figure 1A). We also investigated whether C-CPE$_{194-319}$ (referred to as C-CPE hereafter) is useful for claudin-4-targeted cancer therapy.

Results and Discussion

L cells, which are a mouse fibroblast cell line, do not express any claudins. Therefore, we investigated the cytotoxicity of C-CPE-PSIF in claudin-4-expressing L cells (CL4/L cells). C-CPE-PSIF caused dose-dependent cytotoxicity in CL4/L cells, reaching >90% cell death at 10 ng/ml. In contrast, even at 20 ng/ml, PSIF was not cytotoxic to CL4/L cells (13). C-CPE-PSIF showed specific toxicity in CL4/L cells, and pretreatment of the cells with C-CPE attenuated the C-CPE-PSIF-induced cytotoxicity, indicating that C-CPE-PSIF may interact with claudin-4 via its C-CPE domain (13).

Claudin-4 is expressed in tissues including the lung, intestine, liver, and kidney. Most claudins in normal cells are contained in TJ complexes, whereas the localization of claudin is deregulated in some cancers. C-CPE-PSIF may recognize the deregulated localization of claudin-4. Confluent Caco-2 cells form a polarized cell monolayer with well-developed TJs, and they are frequently used as a model of polarized cells. Confluent Caco-2 cells express more claudin-4 than pre-confluent cells; however, C-CPE-PSIF was more toxic in the pre-confluent cells with fewer TJs (47% cell death at 5 ng/ml) than in the confluent cells with well-developed TJs (40% cell death, even at 200 ng/ml) (13).

Early events in epithelial carcinogenesis are deregulation of cellular polarity and loss of TJ structures. We examined whether the sensitivity of cells to C-CPE-PSIF is affected by their cellular polarity using Caco-2 monolayer cell sheets grown on the membrane in Transwell chambers. The Caco-2 monolayer cells exhibit a well-differentiated brush border containing TJs on the apical surface, and they are frequently used as an epithelial cell sheet model. After the addition of C-CPE-PSIF to the apical or basolateral compartment of the Transwell chamber, we assessed the TJ barrier function of the cell sheets by measuring transepithelial electric resistance (TER). When C-CPE-PSIF was added to the apical compartment, TER was not affected for 48 h. In contrast, the addition of C-CPE-PSIF to the basolateral compartment caused a significant and dose-dependent reduction in TER. Furthermore, the addition of C-CPE-PSIF to the basolateral compartment, but not the apical compartment, increased the amount of released lactate dehydrogenase, a marker of cytotoxicity (13). These results indicate that C-CPE-PSIF has specific effects based on the cellular density and polarity.

We examined the antitumor activity of C-CPE-PSIF in 4T1 cells, a mouse breast cancer cell line that expresses claudin-4. To clarify the antitumor activity of the claudin-4-targeting molecule (C-CPE-PSIF), we prepared a fusion protein of PSIF with mutant C-CPE, in which Tyr306 and Leu315 (critical residues for the interaction between C-CPE

and claudin-4) were changed to alanines, resulting in C-CPE$_{Y306A/L315A}$-PSIF (14). C-CPE-PSIF mediated dose-dependent cytotoxicity in 4T1 cells, reaching 63% cell death at 100 ng/ml. In contrast, C-CPE$_{Y306A/L315A}$-PSIF was not cytotoxic even at 500 ng/ml, indicating that the cytotoxicity of C-CPE-PSIF in 4T1 cells may be mediated by its binding to claudin-4. To investigate the in vivo antitumor activity of C-CPE-PSIF, 4T1 cells (2 x 10^6 cells) were inoculated into the right flank of mice on day 0. Vehicle, C-CPE, C-CPE-PSIF or C-CPE$_{Y306A/L315A}$-PSIF at a dose of 5 μg/kg was intratumorally injected on days 2, 4, 7, 9, 11, and 14. C-CPE-PSIF significantly suppressed tumor growth, and the tumor volume in the C-CPE-PSIF-treated group was 36% of that in the vehicle-treated group on day 16. In contrast, C-CPE and C-CPE$_{Y306A/L315A}$-PSIF, which lacked claudin-4-binding activity, had no effect on tumor growth, indicating that the antitumor activity of C-CPE-PSIF may depend on claudin-4 targeting (13).

We previously investigated the functional domains of C-CPE and found that the 16 C-terminal amino acids of C-CPE are involved in claudin-4 binding; we also found that the claudin-4 affinities of the N309A mutant, which contains Ala instead of Asn at position 309, and the S313A mutant, which contains Ala instead of Ser at position 313, were greater than that of C-CPE (14, 15). To improve the claudin-4-targeting molecule, we prepared C-CPE$_{S313A}$-PSIF and C-CPE$_{N309A/S313A}$-PSIF (Figure 1A). C-CPE$_{S313A}$-PSIF and C-CPE$_{N309A/S313A}$-PSIF were more cytotoxic than C-CPE-PSIF in CL4/L cells (Figure 1B). We are currently investigating the antitumor activity of these mutants and developing other C-CPEmutant-PSIF constructs with greater cytotoxicity. To develop novel methods of tumor diagnosis and therapies that target the initial stage of malignant transformation, we are also developing novel claudins binders, in addition to optimizing C-CPE, the conventional claudin-binder.

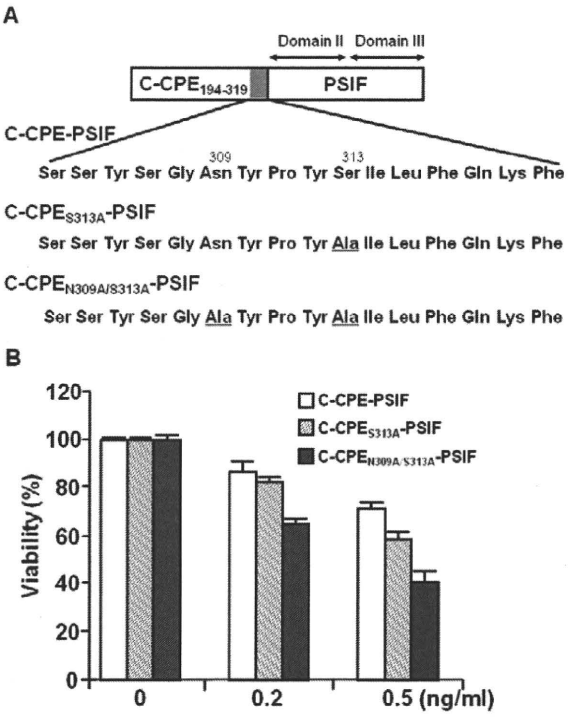

Figure 1. Cytotoxicity of C-CPE-PSIF fusion proteins (A) Schematic illustration of C-CPE-PSIF fusion proteins. C-CPE is the C-terminal fragment of CPE corresponding to amino acids 194-319. The dark area indicates the putative claudin-4-binding region (15). Changing Asn to Ala at position of 309 or Ser to Ala at position of 313 improved the affinity of C-CPE to claudin-4 (14). C-CPE$_{S313A}$ or C-CPE$_{N309A/S313A}$-fused PSIF was also prepared. PSIF contains domain II (the critical domain for the escape of the toxin from the endosome to the cytosol) and domain III (the critical domain for the inhibition of protein synthesis) of *Pseudomonas* exotoxin. (B) Cytotoxicity of C-CPE-PSIF. CL4/L cells were treated with the C-CPE-PSIF fusion proteins at the indicated concentration for 24 h. The cellular viability was measured by a WST-8 assay kit, according to the manufacturer's instructions (Nacalai Tesque, Kyoto, Japan). Viability (%) was calculated as a percentage of the vehicle-treated cells. The data represent the mean ± SD of three independent experiments.

Perspective of claudin-targeted tumor therapy

Approximately 7.6 million people worldwide die from cancer each year, and 90% of malignant tumors are derived from epithelial tissues (16) (http://www.reuters.com/article/healthNews/idUSN1633064920071217).

Cancer cells grow slowly during the very early stage of malignant transformation, after which they grow exponentially and form tumor tissues. Tumors that reach a mass of 10^{12} cancer cells lead to death. Diagnosable cancer tumors contain at least 10^9 cells, and tumors with 10^9-10^{12} cells are subject to cancer therapy. An important goal in cancer therapy is improving the ability to detect tumors containing less than 10^9 cells so that they can be more successfully treated.

Epithelial tissues are characterized by specific cellular polarity. The establishment and maintenance of cell polarity involve many processes, including signaling cascades, membrane trafficking events and cytoskeletal dynamics, and relies on the apical junctional system, TJs (17, 18). TJs seal the intercellular space between adjacent cells and regulate the solute movement across epithelial